5-HT_{2A}-mediated signaling regulates spontaneous waves and 5-HT cell number in the embryonic mouse hindbrain

Lauren Elizabeth Hood

A dissertation

submitted in partial fulfillment of the

requirements for the degree of

Doctor of Philosophy

University of Washington

2019

Reading Committee:

Martha Bosma, Chair
David Perkel
Bill Moody

Program Authorized to Offer Degree:
Neuroscience

University of Washington

Abstract

5-HT_{2A}-mediated signaling regulates spontaneous waves and 5-HT cell number in the embryonic mouse hindbrain

Lauren E. Hood

Chair of Supervisory Committee:

Professor Martha Bosma

Biology

The mouse hindbrain experiences waves of spontaneous depolarizations early in the development of the nervous system. Hindbrain cells along the ventral midline of the neural tube participate in waves for three days with no known functional purpose. The window of activity temporally coincides with the neurogenesis of the hindbrain's serotonergic population. The Bosma lab has previously implicated serotonin (5-HT) signaling in regulating hindbrain activity. The present study has verified through calcium imaging the central role of 5-HT_{2A} signaling in the initiation of spontaneous events. Additionally, in attempt to discover a functional role for spontaneous activity (SA) in hindbrain development, hindbrains were subjected to 24-hours of 5-HT_{2A} receptor antagonists to disrupt SA *in vitro*. On average, a 40% reduction in the number of 5-HT+ cells was found in brains cultured with 5-HT_{2A} receptor antagonists. Interestingly, 5-HT+ cell numbers were only reduced when cultured during the window of neurogenesis; cultures during the 24-hours post-specification exhibited no change in 5-HT+ cell numbers. To

determine whether this reduction was resultant of disrupted SA or disrupted serotonergic signaling, hindbrains were cultured in mibefradil, a T-type calcium channel antagonist known to stop SA. No decreases in 5-HT+ cell numbers were observed, suggesting signaling via 5-HT_{2A} receptors regulates 5-HT cell numbers. No changes were detected in the amount of the other neural population generated in the same progenitor domain during the same developmental window, the visceral motor neurons. Collectively, these data suggest 5-HT_{2A} signals during neurogenesis are important for the appropriate development of 5-HT neurons.

Table of Contents

List of figures and tables

Glossary

E: embryonic day, or the number of days post conception

r: rhombomere

5-HT: 5-hydroxytryptamine or serotonin

5-HT_{2A}R: serotonin 2A receptor

SA: spontaneous activity

Ca^{2+}: calcium

Tph2: tryptophan hydroxylase 2

VMN: visceral motor neuron

VMAT2: vesicular monoamine transporter 2

MAOA: monoamine oxidase A

Sert: serotonin reuptake transporter

GPCR: G-protein coupled receptor

K_i: the inhibitor constant

IHC: immunohistochemistry

Acknowledgements

I'd like to thank my family and friends for their love and support. I would not be here without you all.

I. Introduction

Development of the mammalian hindbrain

The mammalian hindbrain is an evolutionarily ancient structure derived from the rhombencephalon consisting of the pons, medulla and cerebellum. It constitutes a large portion of the brainstem, excluding only the midbrain. Eight of the 12 cranial nerves have roots within the hindbrain (Moens & Prince, 2002). Sensory tracts ascending to the thalamus as well as motor pathways descending to the spinal cord also fasciculate through the hindbrain (Nolte & Krumlauf, 2007). The structures within the hindbrain are collectively responsible for controlling autonomic functions such as heart rate, respiration and brain arousal (Moens & Prince, 2002).

This dissertation focuses on the embryonic stages of hindbrain development in mice. As part of the central nervous system (CNS), the rhombencephalon forms from the neuroepithelium of the gastrula. The lateral edges of the neural plate fold and fuse together during neurulation to form a tube, beginning near the hindbrain at embryonic day 8.5 (E8.5) and extending towards the forebrain and spine until completion around E10.5 (Ybot-Gonzalez et al., 2007). In human embryos, neurulation occurs during the latter half of the first month of gestation, from E18-30 (Lobo, 2008). The neural tube is the precursor of the brain and spinal cord (Ybot-Gonzalez et al., 2007). As new cells are generated and the neural tube thickens, a layer called the ventricular zone forms lining the lumen of the tube, where proliferation continues (Nicholls, Martin, Wallace, & Fuchs, 2001; Nolte & Krumlauf, 2007; Sanes, Reh, & Harris, 2012). The dorsal-most region (toward the back) of the neural tube, where the neural folds have fused, is called the roof plate and the most ventral region (toward the belly), relevant to the current project, is called the floorplate (Figure 1) (Ribes & Briscoe, 2009).

The cells comprising the floorplate have historically been categorized as radial glia-like, responsible for acting as neural organizers though not neurogenic themselves (Bonilla et al., 2008; Kingsbury, 1920; Nicholls et al., 2001). However, more recent studies have determined that floorplate cells are not a homogenous glial population, containing a variety cell types including neural precursors and immature neurons (Bonilla et al., 2008). The floorplate cells of the midbrain can function directly as progenitors, similar to non-floorplate radial glia in the ventricular zone of other brain regions, to produce dopamine neurons (Bonilla et al., 2008; Ever & Gaiano, 2005; Ono et al., 2007). These neurogenic capabilities have not yet been documented in floorplate cells of the hindbrain or spinal cord (Jessell, 2000; Nouri et al., 2015; Ono et al., 2007).

Between the roof and floor plates, along the dorsal-ventral axis within the walls of the neural tube, distinct domains of multipotent progenitors form to generate all the types of neurons and glia needed to complete the CNS (Figure 1). The ventral domains are established primarily through a concentration gradient of the morphogen sonic hedgehog (Shh) released by the floorplate and notochord that activates different profiles of transcription factors in progenitors (Ribes & Briscoe, 2009; Sanes et al., 2012). Opposing gradients of other morphogens (i.e. bone morphogenic proteins (BMPS) and Wnts from dorsal domains) also contribute to domain patterning (Nicholls et al., 2001; Sanes et al., 2012). While the progenitor domains span the length of the neural tube, they can produce different classes of neurons depending on their location and the morphogenic climate along the anteroposterior axis. For example, a p3 progenitor in the spinal cord will create different neurons than p3 progenitors

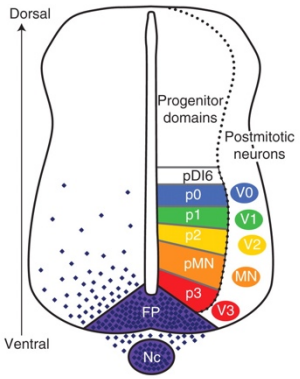

Figure 1: Progenitor domains in neural tube. Only ventral progenitor domains are pictured in this coronal section. Shh shown in purple. Nc=notochord, FP=floorplate. (Ribes & Brsiscoe, 2009)

in the hindbrain or midbrain. The same domains can also produce multiple cell types throughout different stages of development, due to changes in environmental cues and gene expression as the embryo ages.

Throughout development, the hindbrain experiences important transitory phenomena. One early example involves a morphological transformation unique to the hindbrain lasting from E8.5-11.5 (Marti Bosma presentation). The rhombencephalon is temporarily divided into sections called rhombomeres that are similar in appearance to vertebrae. There are 7 distinct rhombomeres segmenting the rostrocaudal axis of the hindbrain, with rostral referring towards to head and caudal towards the tail of the animal. During this phase, cells cannot travel between segments due to temporary cell adhesion restrictions (Philippidou & Dasen, 2013). In the context of the serotonergic literature to be discussed later, the rhombomeres are typically clustered into two groups; r1-3 are considered to be rostral and r5-7 are considered caudal relative to each other, with r4 as a midpoint barrier (Deneris & Gaspar, 2018; Kiyasova & Gaspar, 2011). There is some ambiguity regarding the inclusion of an 8th rhombomere, as this is an elongated transition area to the spinal cord that is often omitted from the caudal group (Sturgeon et al., 2011).

Rhombomeres are defined by borders of *Hox* gene expression; the *Hox* transcription factor family is highly conserved across species and crucial for specifying the anteroposterior fate of vertebrates tissues (Nolte & Krumlauf, 2007). Differential *Hox* gene expression is in part established by retinoic acid (RA) and fibroblast growth factor (FGF) gradients along the neural tube. The combination of *Hox* genes expressed within each rhombomere induces different transcriptional cascades to help dictate neuronal identity (Nolte & Krumlauf, 2007). For example, while every rhombomere produces motor neurons in the pMN domain (Figure 1), trigeminal motor neurons only form in r2 and r3 and facial motor neurons only in r4 and r5 (Graham, Butts,

Lumsden, & Kiecker, 2014; Sanes et al., 2012). r4 is the only rhombomere to express the *Hoxb1* gene, which later effects the phenotype of cells made from hindbrain p3 progenitors by preventing production of the serotonin lineage (Pattyn et al., 2004). Another developmental process of particular importance to this dissertation is a period distinguished by waves of spontaneous excitation traveling through the hindbrain neural network.

Spontaneous Activity

1. Origins and functions

Spontaneous activity (SA) is a transient phenomenon that is common in developing neural tissue (i.e. retina, cochlea, cortex, hippocampus, midbrain, hindbrain, spinal cord) where neurons and neural precursors are excitable in the absence of external stimuli (Bortone & Polleux, 2009; McCabe, Easton, Lischalk, & Moody, 2007; Meister, Wong, Baylor, & Shatz, 1991; Yang, Hanganu-Opatz, Sun, & Luhmann, 2009). The term "spontaneous" is not meant to insinuate activity occurs completely at random without pattern; rather, it refers to the activation of neurons independent of the sensory input or motor responses that evoke action potentials in mature neurons. This chemical and electrical activity can occur at both the cellular and population level. Each spontaneous depolarization event is associated with a rise in intracellular calcium (Ca^{2+}) concentrations (De Lima, Gieseler, & Voigt, 2009; Moruzzi, Abedini, Hansen, Olson, & Bosma, 2009). Brain regions can experience multiple types of SA over the course of development, with patterns that evolve alongside the neurons that create them. For example, embryonic neurons in the mouse hippocampus experience SA in the form of plateau potentials within small clusters of neurons but shift after birth to participate in expansive depolarizing waves across larger areas

(Blankenship & Feller, 2009). The current project focuses on coordinated firing in the form of synchronous waves.

Developing neural tissues generate synchronous waves of SA due to the intrinsic properties of immature neurons and interactions within emerging networks (Blankenship & Feller, 2009; Lischalk, Easton, & Moody, 2009). Understanding the origin of SA, whether from the behavior of a subset of neurons or the network as a whole, is important for understanding the mechanisms underlying the activity (Lischalk et al., 2009). The presence of pacemaker neurons or regions are known initiate synchronous events within the mouse cortex, hippocampus and cerebellum. Pacemakers are excitable neurons, with unstable membrane potentials prone to depolarization, that trigger neighboring cells to fire and generate waves. The neocortex has two distinct pacemaker populations, in the septal nucleus and the piriform cortex, that initiate separate GABAergic and glutamatergic cortical waves postnatally (Easton et al., 2014). Retinal waves are dependent on the ability of the starburst amacrine interneurons to spontaneously depolarize, which includes mediation via network interactions. The more amacrine cells in the network that have recovered from the slow after-hyperpolarization period following an event, the more likely a wave will occur (Blankenship & Feller, 2009). The SA in the spinal cord, on the other hand, does not definitively rely on a pacemaker region. Some reports suggest cholinergic motor neurons act as pacemakers, as these are the first neurons activated in an event, while others argue the dynamics within the circuit are more essential for wave initiation. Excitatory GABA, acetylcholine and glutamate are all continually released from immature neurons and the network must collectively recover from an event before the ongoing synaptic excitation can trigger another wave.

One common contributor to the presence of SA in early neural development is a general lack of inhibition. The classic inhibitory neurotransmitters of mature brains, GABA and glycine,

function as excitatory signals throughout embryonic and early postnatal mouse development (Easton et al., 2014). This is due to the fact that immature neurons have higher intracellular concentrations of chloride (Cl^-) compared to mature neurons, meaning Cl^- will follow its concentration gradient out of the cell when GABA receptors are activated to cause depolarization. The internal concentration of Cl^- decreases as cells mature and upregulate the expression of Cl^- transporters. Excitatory GABA signaling is important for activity propagation in the spinal cord, hippocampus and neocortex. SA dissipates in these systems once GABA becomes fully inhibitory (Blankenship & Feller, 2009; Easton et al., 2014; Moody & Bosma, 2005).

SA can travel through neural circuitry at early stages of development prior to the formation of conventional synapses. Direct connections, through gap junctions and synaptic transmission, can be temporarily established to pass excitation through a population of cells that does not form functional synapses in maturity (Blankenship and Feller, 2009). Starburst amacrine cells in the retina interconnect to form an excitable network dependent on acetylcholine and cease to maintain these excitatory links as the retina matures (Blankenship & Feller, 2009). Purkinje cells of the cerebellum synapse heavily with neighboring Purkinje cells during development, and while some persist to adulthood, the density of these collaterals are greatly reduced once SA terminates. The cochlea and spinal cord also experience fleeting connections to sustain SA (Blankenship & Feller, 2009).

SA regulates many developmental processes vital to the appropriate formation of the nervous system. The expression of ligand-, voltage-, and Ca^{2+}-gated ion channels can be regulated by SA. For example, in the developing mammalian neuromuscular junction, the subunits of acetylcholine receptors expressed is activity-dependent; the fetal form of the receptor is suppressed by electrical activity from nerves innervating muscles (Moody & Bosma, 2005). Voltage-gated

sodium ($Na^{+)}$ channels are also regulated in an activity-dependent fashion. Early in development, activity in cortical and hippocampal neurons leads to an internalization of Na^+ channel proteins and downregulation of Na^+ channel alpha-subunit mRNA. Conversely, outward potassium (K^+) currents are increased in response to SA through the upregulation of voltage-gated K^+ channels (Kv1.1, Kv1.2 and Kv1.4) (Moody & Bosma, 2005). In this way, SA contributes to its own termination by ultimately promoting the expression of channels that lead to membrane hyperpolarization and reduction of spontaneous excitation, helping transition the brain to a more mature state.

The appropriate wiring of neural circuits is influenced by SA, with documented effects on axonal pathfinding and synapse formation. In the retina, starburst amacrine cells spontaneously generate waves of activity, which are then transmitted by retinal ganglion cell axons to post-synaptic thalamic neurons during synaptogenesis. Disruption of these waves results in inaccurate retinotopic maps encoded in the lateral geniculate nucleus of the thalamus (Shatz & Stryker, 1988). SA is also important for axonal pathfinding in the developing spinal cord, as slowing the frequency of waves prevents motor neurons from innervating their correct targets (Kastanenka & Landmesser, 2013).

Some forms of cellular migration are also modulated by SA. Cells are not typically born in their final locations and require passage from ventricular/progenitor zones to their proper placement in the cytoarchitecture (Komuro & Rakic, 1996). Komuro and Rakic (1996) have shown that migrating granular neurons in the cerebellum exhibit intrinsic SA. The frequency and amplitude of these spontaneous Ca^{2+} transients are positively correlated with the rate of migration in cultured slices from the first postnatal week. When these aspects of intrinsic Ca^{2+} transients increase, so do migration rates; conversely, reductions in Ca^{2+} spikes correlate to slower cell

movements. These intrinsic Ca^{2+} transients are independent from neighboring cells, and are not the same type of SA as the waves that propagate synchronously through networks. These two different types of SA can have opposing effects on neuronal migration. Synchronous waves of cortical SA reduces migration in inhibitory interneurons (De Lima et al., 2009; Easton et al., 2015). The majority of cortical interneurons are born in the ganglionic eminences and migrate laterally into the neocortex (De Lima et al., 2009). These cells present intrinsic SA independent from neighboring cells during their migratory period prior to the onset of cortical wave activity. The onset of cortical waves overlaps with the cessation of interneuron migration. The number of interneurons migrating declines as the number participating in cortical wave activity increases. Those that participate do not migrate, suggesting network activity suppresses interneuron migration (De Lima et al., 2009).

SA has also been implicated in playing a role in proliferation and cell survival. In cultured cortical slices, blocking SA with tetrodotoxin increased the number of subsequent GABAergic interneurons that develop (De Lima et al., 2009). Antagonists to GABA and glutamate receptors also increased general proliferation rates. However, these antagonists did not affect interneuron neurogenesis, suggesting the SA and not the lack of neurotransmission was responsible for the increase in the GABAergic population. This study provides direct evidence that SA can influence developmental neurogenesis, which is relevant to the current dissertation. Activity is also shown to be important for the survival of these GABAergic interneurons, suggesting SA is important for both the genesis and maintenance of a neural population (De Lima et al., 2009). Despite extensive evidence that SA is important for normal development, the role of neuromodulators beyond GABA and glutamate in shaping this activity, and therefore affecting development, is unclear.

2. SA in the hindbrain

In the hindbrain, two distinct patterns of SA have been reported during the same developmental window of E11.5-13.5 (Momose-Sato, Nakamori, & Sato, 2012). Sato and colleagues report an embryo-wide wave of depolarization, deemed "the depolarization wave", that begins in the spinal cord and spreads globally throughout the entirety of the neural tube, including the hindbrain. This group has described similar depolarization waves in chick and rat embryos. A second form of SA has also been reported in the hindbrain, by both the Sato group and the Bosma group (Hunt et al., 2006; Hunt et al., 2005; Momose-Sato et al., 2012). The latter form arises within the hindbrain on the ventral midline as opposed to the spinal cord. The two forms of activity are also driven by different mechanisms, with the midline activity dependent on a single population of neurons that are not essential for the depolarization wave (Momose-Sato et al., 2012). Because of these differences in initiation zones, propagation patterns, and neurotransmitter involvement, the two forms of activity are suggested to be independent occurrences. However, the isolation of the hindbrain in the open-book preparation used for all Bosma lab experiments could possibly prevent the detection of midline events participating in large scale depolarization waves (Figure 8). The lack of serotonergic modulation in Sato's depolarization wave may be due to interference from other neurotransmitter systems, which would not be present in experiments utilizing the isolated open-book preparation. Regardless, the function of waves in the hindbrain is unknown. Both reports of activity have also terminated before the pons, medulla and cerebellum develop into discrete structures; the cerebellum later experiences its own patterns of SA (Blankenship & Feller, 2009).

The Bosma lab has pioneered research specifically on the midline-driven SA in the mouse hindbrain. Measured in an isolated open-book preparation (Figure 8), only asynchronous events in single cells throughout the hindbrain are observed from E9.5-10.5. Cells then participate in synchronous activity that propagates in waves along the ventral midline of the neural tube. These waves originate on the rostral midline at E11.5 around r2 and initially propagate in rostrally, caudally and laterally (Figure 2A&B). The area of propagation becomes increasingly restricted as

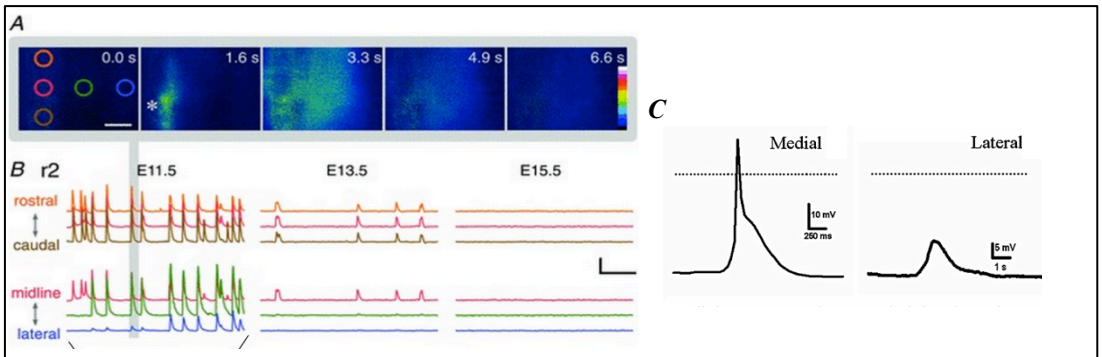

Figure 2: Midline SA in the hindbrain. **A**. Heat map of a calcium event at E11.5. Colored circles represent ROIs along the midline (orange, pink, brown) and lateral tissue (green, blue), from which average fluorescence intensity over time is measured. The wave initiates at the asterisk and propagates to all regions. **B**. Representative calcium traces that correspond to circles in A. By E13.5, the waves do not propagate to lateral tissue. By E15.5, activity is absent. **C**. Patch clamp recording of SA at Ell.5. Only midline cells (left) have biphasic events. The dashed line marks 0mV (**A** and **B** from Watari et al., 2013; **C** unpublished data from Bosma lab).

development progresses, with the lateral tissue retracting first, until the ultimate cessation of SA by E15.5 (Watari, Tose, & Bosma, 2013).

The observed spontaneous events, detected through Ca^{2+} imaging and patch clamping, are not conventional action potentials. They are slower (0.3-1 sec duration) without significant afterhyperpolarization; they do not always overshoot 0mV and are graded in amplitude. The cells of the midline exhibit higher amplitudes of depolarization than lateral cells (Figure 2C). At E11.5, there are T-type calcium channels (Cav3.3) expressed at sufficient density to generate spontaneous activity in the midline cells but little expression in the lateral cells; these channels have substantial window current. The resting membrane potential of the rostral midline cells is initially depolarized

at E11.5, averaging around −40.2 ± 3.6 mV from E11.5-E13.5, setting them to the appropriate voltage range to activate the Cav3.3 channels (Watari et al., 2013). Rostral midline cells have high resistance so that calcium channel opening leads to substantial depolarization. The midline cells are also coupled through gap junctions at an average of six cells, as quantified by diffusion of neurobiotin; lateral cells are more highly coupled at an average of 23 cells. Over developmental time, membrane hyperpolarization via upregulation of potassium conductance in a strict spatiotemporal order is responsible for retraction of the regions participating in waves. The lateral cells hyperpolarize first, and are subsequently the first cells to withdraw from wave participation (Figure 2B).

While many neurotransmitters modulate the frequency of midline SA, the Bosma lab has shown 5-HT is necessary for the propagation of waves. Bath application of ketanserin, a non-specific 5-HT_2 receptor family antagonist, completely and reversibly arrests spontaneous events (Hunt et al., 2006; Hunt et al., 2005). Interestingly, the application of exogenous 5-HT does not change the frequency of SA, suggesting a ceiling effect of endogenous 5-HT action (unpublished data). Treatment with cocktails of antagonists of $GABA_A$, $GABA_B$, metabotropic and ionotropic glutamate, D1, D2, noradrenaline, substance P, and muscarinic and nicotinic acetylcholine receptors failed to block SA (Hunt et al., 2006). This differs from the depolarization wave characterized by Sato, which is initially dependent on activation of nicotinic acetylcholine receptors and later driven by glutamate. Sato also found that GABA contributed to wave activity as an excitatory modulator from E11-12, but switched to regulate the wave through inhibition by E14. This is an early transition of GABA from excitatory to inhibitory transmission, as this switch is still occurring in cerebellar and neocortical SA postnatally (Blankenship & Feller, 2010; Easton et al., 2014).

Pharmacologically, 5-HT neurons are linked to midline waves of SA in the hindbrain. Developmentally, the window of observed SA temporally coincides with 5-HT neurogenesis. The onset of activity (E11.5) is 24 hours after differentiation begins for rostral 5-HT cells. By E11.5, there is abundant 5-HT present throughout the newly born population, as verified through immunohistochemistry (Deneris & Gaspar, 2018; Hunt et al., 2005). Spatially, the 5-HT neurons lie within the p3 domain adjacent to the spontaneously active midline (Figure 3). However, beyond these facts tying neural population to electrical phenomenon, the relationship between 5-HT signaling and hindbrain SA remains largely unstudied.

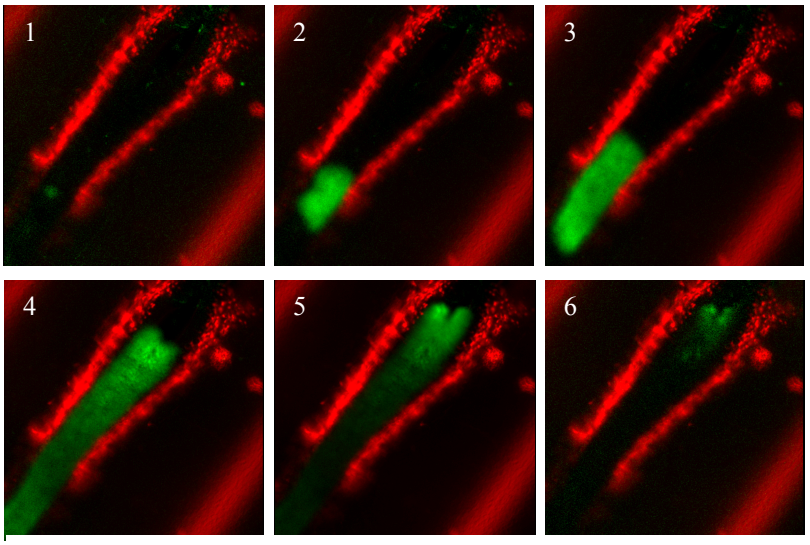

Figure 3: Serotonin neurons and calcium imaging. Localization of 5-HT neurons (genetically labeled with Tdtomato in red) in close proximity to a spontaneous wave propagating rostrally and caudally along the midline (in green). The event begins in box #1 and ends in #6. Unpublished data by Jesse Miles.

Serotonin neurons

5-HT is a monoamine neuromodulator. The effect of 5-HT signaling is not inherently excitatory or inhibitory like the classical neurotransmitters GABA and glutamate. Rather, 5-HT alters the excitability of a neuron depending on the type of receptor it activates (Deneris & Gaspar, 2018; Shen, Kozell, & Johnson, 2007). The majority of 5-HT in the mammalian body is located in the enteric nervous system of the gut, though the brain also synthesizes its own separate supply for neurotransmission. In the brain, 5-HT is derived from the amino acid tryptophan through a

chemical conversion catalyzed by aromatic amino acid decarboxylase (Aadc) and the rate-limiting enzyme tryptophan hydroxylase 2 (Tph2) (Deneris & Gaspar, 2018).

The mature serotonergic system in the CNS projects throughout the entire brain, influencing a broad range of behavior and autonomic function. 5-HT cell bodies reside within the seven raphe nuclei of the brainstem (Lesch & Waider, 2012). The 5-HT neurons from caudal rhombomeres innervate the brainstem and spinal cord, while neurons from the rostral rhombomeres innervate everything else. The dorsal raphe nucleus (DRN) is composed of 50% serotonergic neurons originating from r1 and r2 that project to the basal ganglia, amygdala, hippocampus, prefrontal cortex, and thalamus (Deneris & Gaspar, 2018). 5-HT cells from r2 also form the median raphe nucleus (MRN) and project to the suprachiasmatic nucleus to regulate circadian rhythms, the thalamus to influence sleep, and the hippocampus and entorhinal cortex to impact memory (Canli & Lesch, 2007). Appetite and digestion, social behaviors like aggression and maternal care, processing reward, sexual desire, learning, mood, temperature regulation, and breathing are all processes affected by serotonergic modulation (Deneris & Gaspar, 2018). In light of its expansive sphere of signaling, dysregulation of the 5-HT system has been implicated in many diseases, including addiction, mood disorders, autism and schizophrenia (Deneris & Wyler, 2012; Lesch & Waider, 2012; Muller et al., 2017). The ability of one population of neurons to assert power over both the development and maintenance of so many aspects of a functioning nervous system attests to their importance. The current project involves the generation of the 5-HT neurons.

1. 5-HT neurogenesis

Hindbrain progenitors give rise to different classes of neurons, including motor neurons, noradrenergic neurons and all of the brain's serotonergic neurons (Bosma, 2010). The serotonergic neurons are generated specifically from the p3 pool of progenitors flanking the floorplate of the developing neural tube (Figure 1). The high ventral concentration of Shh from the floorplate and notochord specifies the p3 domain through the induction of the Nkx2.2 transcription factor (Jacob et al., 2007). 5-HT neurons are not generated in Nkx2.2$^{-/-}$ mice (Briscoe et al., 1999). p3 progenitors along the rostral-caudal axis of the hindbrain undergo serotonin (5-HT) neurogenesis sequentially, with the rostral regions commencing before the caudal regions. At this early stage in development, the hindbrain is still segmented into rhombomeres (Figure 4). The most rostral rhombomeres generate the rostral group of 5-HT cells commencing at E9.5, with the genesis of the caudal group beginning at E11.5 in the caudal rhombomeres. r4 progenitors are not included as participants in 5-HT neurogenesis (Deneris & Gaspar, 2018). One paper does report finding a small population of serotonergic neurons in the r4 region postnatally, though no explanation was provided regarding the genesis of this population (Alonso et al., 2013).

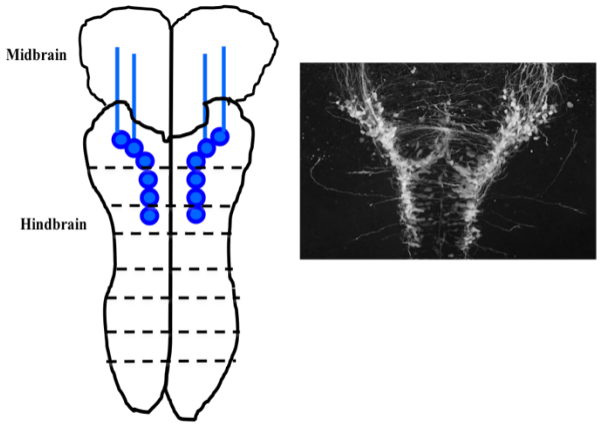

Figure 4: Morphology of rostral 5-HT neurons in open book conformation. 5-HT immunostain of whole mount E11.5 hindbrain (right) with schematic of rostral 5-HT population within rhombomeres, denoted by dotted lines (left). (Unpublished data from this dissertation).

The p3 progenitors in the hindbrain are tri-potent with the competency to produce motor neurons, 5-HT neurons and oligodendrocyte precursors (Deneris & Gaspar, 2018). Visceral motor neurons (VMN) are generated first, from E9.5-10.5, followed closely by 5-HT neurons (Jacob et al., 2007). The fate of the p3 progeny is largely determined by a spatiotemporal gradient of transcription factors that repress each other (Jacob et al., 2007; Pattyn et al, 2003; Deneris &Wyler, 2012). Phox2b is the transcription factor induced first by Nkx2.2 and Nkx2.9 in the p3 progenitors to direct VMN production (Figure 5). The downregulation of Phox2b is required for the 5-HT phenotype to develop (Pattyn et al, 2004). Phox2b is repressed by Nkx2.2 and Foxa2, a prominent transcription factor for inducing the 5-HT lineage (Deneris & Gaspar, 2018). 5-HT neurons never develop in mice lacking Foxa2 expression (Jacob et al., 2007).

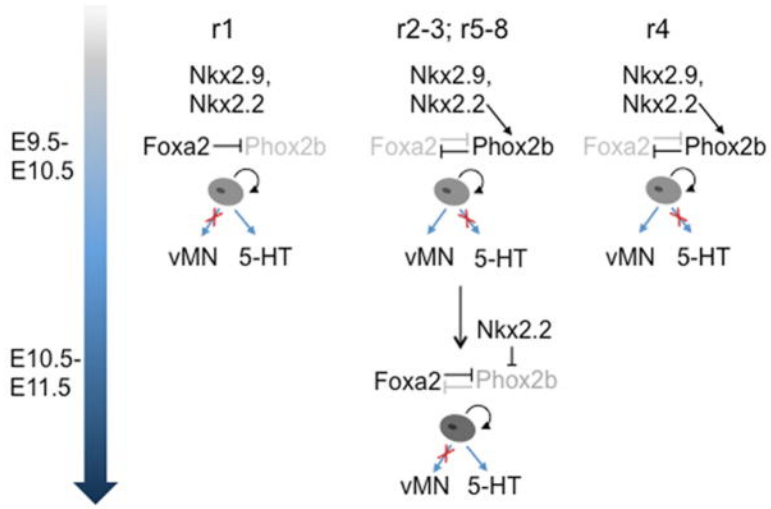

Figure 5: p3 progenitors in the rostral hindbrain produce VMNs and 5-HT neurons. r1 produces 5-HT neurons at E9.5 due to Foxa2 repression of Phox2b. 5-HT production doesn't begin in r2-3 until E10.5. r4 only produces VMNs. (Deneris & Wyler, 2012).

Foxa2 is initially expressed in the floorplate; the expansion of Foxa2 expression into the p3 domain of the hindbrain marks the shift from generating VMNs to 5-HT neurons (Deneris & Gaspar, 2018; Jacob et al., 2007). There are two exceptions to this progression: in r1 and r4. By E9.5, progenitors in r1 already co-express Nkx2.2 and Foxa2 to begin 5-HT neurogenesis (Figure 5). This results in the production of only 5-HT neurons from p3 progenitors in r1. r1 is responsible

for generating 50% of the rostral group of 5-HT neurons (Jacob et al., 2007). The loss of Foxa2 expression in r1 results in ectopic VMN expression (Jacob et al., 2007). Foxa2 is never expressed in r4, where Phox2b expression is maintained by *Hoxb1*, resulting in only VMN production in this region (Pattyn et al., 2004). Foxa2 is expressed in r2-3 starting at E10.5, and is expressed last in r5-7 at E11.5. Therefore, there are three separate 24-hour periods of 5-HT neurogenesis progressing caudally through the hindbrain; in r1 from E9.5-10.5, in r2-3 from e10.5-11.5 and in r5-7 at e11.5-12.5.

A network of other transcription factors is also required for specification of the serotonergic phenotype (Figure 6). Ascl1, also known as Mash, is a basic helix-loop-helix transcription factor expressed with Nkx2.2 in p3 progenitors. Ascl1 has a dual-purpose role in 5-HT neurogenesis: first, Ascl1 acts as a proneural gene necessary for creating neural precursors. Without the expression of a proneural gene, post-mitotic cells cannot differentiate into neural phenotypes. Motor neurons develop normally in Ascl1$^{-/-}$ mice due to the proneural function of Phox2b. However, either Ascl1 or Phox2b is required for hindbrain neurons to develop (Pattyn et al., 2004). The second role of Ascl1 is specific to the specification of monoamine neurons, including noradrengeric and serotonergic phenotypes. No 5-HT neurons develop in Ascl1$^{-/-}$ mice, as Ascl1 is responsible for regulating the downstream genes necessary for 5-HT synthesis (i.e. Pet-1, Lmx1b, and Gata3) (Deneris & Gaspar, 2018; Pattyn et al., 2004).

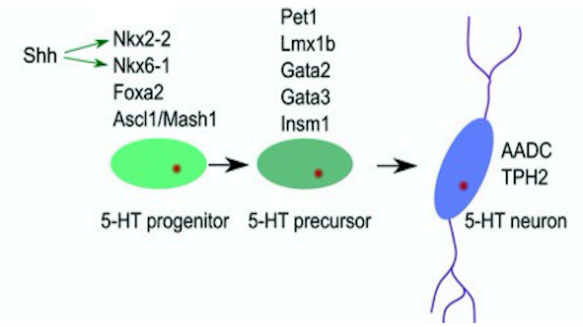

Figure 6: Development of 5-HT neurons. The transcription factor profiles of 5-HT progenitors (left) and precursors (middle) lead to the proteins expressed in mature 5-HT neurons (right). Specification refers to cells reaching the precursor stage, while differentiation refers to cells reaching the mature neuron state. (Smidt and van Hooft, 2013)

Pet-1 is an ETS domain transcription factor expressed downstream of Nkx2.2 and Acsl1 in post-mitotic 5-HT precursor cells (Pattyn et al., 2004). Pet1 is expressed in both 5-HT neurons and glutamatergic neurons (that are Vglut3+ and 5-HT-) in the DRN (Deneris & Wyler, 2012; Haugas, Tikker, Achim, Salminen, & Partanen, 2016; Hendricks, Francis, Fyodorov, & Deneris, 1999). While ectopic expression of Pet-1 alone is insufficient to induce the 5-HT phenotype, Pet-1 expression is a necessary component for the specification, differentiation and maintenance of 70% of the 5-HT lineage (Cheng et al., 2003). Studies suggest the Pet-$1^{-/-}$ subset of 5-HT neurons is phenotypically and functionally divergent (Kiyasova et al., 2011). This subset innervates regions of the brain involved in processing responses to stress, namely the basolateral amygdala, the paraventricular nucleus in the hypothalamus, and the intralaminar thalamic nuclei. In $Pet1^{-/-}$ mice, which causes a reduction of 70% of 5-HT neurons, there are differing reports on behavior; increases and decreases in both fear and anxiety measures from the elevated plus maze have been observed (Hendricks et al., 2003; Kiyasova et al., 2011). Thus, the consensus in the literature is that Pet-1 is necessary for normal anxiety and fear responses.

Another vital regulator of the 5-HT phenotype, activated in parallel to Pet-1, is the *Lim* class homeobox gene Lmx1b (Pattyn et al, 2004; Cheng et al., 2003). 5-HT cells are not specified without Lmx1b expression (Cheng et al., 2003). Floorplate cells, noradrenergic neurons and dopaminergic neurons also express Lmx1b during development. After specification, Lmx1b is also important for the differentiation and survival of 5-HT neurons, maintaining expression in this population throughout adulthood. When Lmx1b expression is eliminated after 5-HT cells have already been generated, through a conditional knock out in Pet-1+ cells only, there is a complete loss of the 5-HT phenotype without impacting the noradrenergic and dopaminergic populations (Zhao et al., 2006).

Interestingly, lower vertebrates have exhibited activity-dependent expression of Lmx1b, and the subsequent specification of the 5-HT lineage (Demarque & Spitzer, 2010). Similar to the mouse condition, SA is observed in the hindbrain during 5-HT specification in *Xenopus laevis* larvae. Around 30% of the active cells tested positive for 5-HT progenitor and precursor markers. Decreasing activity led to an increase in the number of Lmx1b+ cells, while increasing activity had the opposite effect. No change was detected for other progenitor or precursor markers (Demarque & Spitzer, 2010). This activity-dependent effect has not been substantiated in mammalian systems.

The remaining core transcription factors necessary for 5-HT maturation are Insm1, Gata2 and Gata3 (Figure 6). *Insm1*, a zinc-finger gene, regulates the synthesis of monoaminergic neurotransmitters, including serotonin and noradrenaline. Insm1$^{-/-}$ mutants display normal levels of Aadc expression, but diminished Tph2 levels, supporting a role for Insm1 in the differentiation of 5-HT precursors into functional neurons. Insm1 induces Tph2 expression in conjunction with Ascl1, independently of Pet1 and Lmx1b, suggesting the 5-HT neurons persisting in Pet1$^{-/-}$ mice are induced through this pathway (Jacob et al., 2009; Deneris & Gaspar, 2018). However, Ascl1 also plays a vital role in activating Insm1, as it is not expressed in Ascl1$^{-/-}$ mice (Jacob et al., 2009; Deneris & Gaspar, 2018). Therefore Insm1 acts downstream of Ascl1, and together are capable of inducing Tph2 expression. Pet1, Lmx1b and Gata3 are all expressed but at diminished levels without the presence of Insm1, suggesting Insm1 acts upstream of these transcription factors.

Gata2 and *Gata3* are also zinc-finger genes believed to act independently of each other, though both required for the full complement of 5-HT neurons to develop (Deneris & Gaspar, 2018; Haugas et al., 2016). All in all, the transcriptional web encompassing 5-HT neurogenesis is continually evolving. Over the years, there have been some conflicting conclusions regarding the

exact hierarchical order of regulation (Deneris & Gaspar, 2018; Deneris & Wyler, 2012; Kiyasova et al., 2011; Smidt & van Hooft, 2013). The consistent thread in these reviews supports that multiple transcriptional pathways exist for producing the 5-HT phenotype.

2. Morphogenic role of 5-HT in neural development

In addition to its prominent synaptic role as a neuromodulator, 5-HT has been shown to influence many aspects of CNS morphogenesis, or the process of the nervous system developing its shape, in organisms ranging from aquatic mollusks and mammals. Morphogenesis includes proliferation, migration, differentiation and synaptogenesis of developing neurons (Lauder, Tamir, & Sadler, 1988; Lesch & Waider, 2012). The prenatal environment influences fetal 5-HT levels, and therefore neural development. For humans, 5-HT levels in utero can be affected by diet, stress, illness, genetic polymorphisms, medications and drugs of abuse (Daubert & Condron, 2010; Vitalis & Parnavelas, 2003).

Serotonin neurons are one of the first types of neurons created in the brain, and immediately upon differentiation, begin producing 5-HT. This starts as early as E10.5 in the rostral rhombomeres (Bonnin et al., 2011). By Ell.5, there is already robust 5-HT present throughout the rostral hindbrain, which is detectable through immunohistochemistry (Figure 4). Axons from hindbrain 5-HT neurons reach the forebrain around E14.5 and continue innervation throughout the following days. However, low concentrations of 5-HT are already present in forebrain during E10.5-12.5 (Bonnin et al., 2011). When comparing $Pet1^{-/-}$ mice with wild type controls, both strains have comparable concentrations of 5-HT in the forebrain until E16.5, despite the large decrease in hindbrain 5-HT levels in the $Pet1^{-/-}$ condition. After E16.5, 5-HT levels in $Pet1^{-/-}$ forebrains significantly drop. The fetal enteric nervous system also does not produce 5-HT until after E15.5 (Bonnin & Levitt, 2011). These data suggest that serotonergic influence from maternal

and placental sources influences early embryonic development (Deneris et al., 2018; Bonnin et al., 2011). Bonnin et al. (2011) have provided evidence that maternal tryptophan is processed by the placenta to produce the 5-HT supply crucial for the axonal guidance of thalamocortical projections in the embryo. Altering the maternal serotonin transporter (SERT) can impact placental 5-HT and subsequent neural development (Muller et al., 2017).

Placental 5-HT has also been shown to impact migration in neural crest cells (Moiseiwitsch & Lauder, 1995). The effect was found to be dose-dependent in cultured neural crest cells, with low concentrations of 5-HT stimulating migration and higher concentrations failing to do so. Antagonists to only the 5-HT_{1A} receptor prevented the stimulation, suggesting activation of these auto-receptors is important for 5-HT mediated migration. This migration occurs at E9.5, before 5-HT is produced in the embryo, meaning an external source must be supplying the morphogen. Placental inputs of 5-HT dissipate around E16.5 in the cortex, and are replaced by 5-HT from emerging serotonergic afferents (Vitalis et al., 2013).

Interneuron migration is regulated by 5-HT. Pregnant rats were injected daily with DL-P-chlorophenylalanine methyl ester hydrochloride (PCPA), an inhibitor of 5-HT synthesis that is known to cross the placenta, during a prominent cortical development period, E12-E17 (Vitalis et al., 2007). When evaluating the embryos from these dams, embryonic interneurons displayed reduced migration and delayed integration into the cortical plate. Cortical pyramidal neurons were also found to have less complex dendritic arbors (Vitalis et al., 2007). Similarly, depleting 5-HT with PCPA decreased spine density on the dendrites of CA1 neurons in the hippocampus (Alves et al., 2002). An excess of serotonin had the opposite effect on dendritic spines of the postnatal rat hippocampus. Acute injections with an antidepressant to prevent the reuptake of serotonin

resulted in denser and longer dendritic spines in CA1 of the hippocampus (Norrholm & Ouimet, 2000).

In line with these positive effects on dendritic arborization, 5-HT can also have a trophic effect on neurite outgrowth. Culturing rat postnatal thalamic neurons in serotonin-enriched media resulted in increased primary neurite lengths (Lieske, Bennett-Clarke, & Rhoades, 1999). The number of branches and total number of neurites and total neurite lengths also increased. Increases in neurite length also occur with increased serotonin in embryonic mouse thalamic cultures (Persico, Di Pino, & Levitt, 2006). However, opposite effects of 5-HT have also been reported on the same types of neural cultures (Liu & Lauder, 1991). Differences in 5-HT concentration and culture methodology may contribute to these conflicting results.

5-HT has been shown to augment the differentiation of the glutamatergic phenotype in developing cortical slices. A significant increase was found in both the number of glutamatergic neurons and the concentration of glutamate present in cortical cultures that had been supplemented with 5-HT. There was no difference in the amount of proliferation between 5-HT-treated cultures and controls, supporting the role of 5-HT in directing the differentiation stage of neurogenesis (Lavdas, Blue, Lincoln, & Parnavelas, 1997). 5-HT has also acted as neuroprotective against cell death in cortical neurons of mice lacking VMAT2, specifically signaling through 5-HT_2 receptors (Stankovski et al., 2007).

There are many examples of transgenic mice with altered functionality of the serotonergic system. In $Pet1^{-/-}$ mice, as previously mentioned, 70% of the 5-HT population does not differentiate and adult mice exhibit irregular fear and anxiety behavior. When Lmxb is conditionally removed only in Pet1+ neurons, 5-HT neurons are generated as normal until E12.5 (Zhao et al., 2006). At E12.5, there is a noticeable decline in the amount of 5-HT cells which

continues until the mice have lost all of the 5-HT neurons in the CNS. Zhao et al. (2006) report the conditional Lmxb$^{-/-}$ mice exhibited no gross morphological abnormalities in brain structures outside of the raphe nuclei, with similar levels of dopamine and norepinephrine in the brain as wild type mice. The mice also experienced normal locomotor behavior as adults. It is possible developmental abnormalities in both brain structure and behavior existed that were not detected by the tests used in this paper.

Increasing serotonin concentrations during development contributes to gross morphological changes. Deleting the mechanism for degrading serotonin, monoamine oxidase A (MAOA), increases the concentration of 5-HT nine-fold throughout development. These mice are very aggressive, and did not have the cytoarchitectural barrels that normally form in the somatosensory cortex due to aberrant growth of thalamocortical axons (Vitalis et al., 2003). However, other monoamines like norepinephrine were also elevated, though to a lesser degree (Cases et al., 1995). More recent studies selectively delete MAOA in 5-HT neurons and showed that this aggression phenotype was a direct result of the selective increase in 5-HT concentration (Persico et al., 2003; Vitalis et al., 2002; Bou-Flores et al., 2000). A similar result is achieved from knocking out the serotonin reuptake transporter (SERT), which would prevent 5-HT removal from the synapse after release. Sert$^{-/-}$ mice also experience less cell death in telencephalon neurons, suggesting a role for 5-HT in promoting cell survival (Gaspar et al., 2003).

Non-monoaminergic neurons transiently uptake serotonin during development (Gaspar et al., 2003). This phenomenon is highly conserved across species, occurring even in marine crustaceans (Gaspar et al., 2003). After 5-HT neurons are generated in the hindbrain, 5-HT can be detected inside neurons throughout the thalamus, hypothalamus, cortex, retina, and super olivary nucleus (Cases et al., 1998; Hansson, Mezey, & Hoffman, 1998; Lauder et al., 1988;

Lebrand et al., 1998; Upton et al., 1999). The neurons accumulating 5-HT in these regions temporarily express Sert and VMAT2, in order to capture 5-HT and package it into vesicles, but do not express the enzymes necessary for 5-HT production (Aadc and Tph2). The function for this phase of 5-HT hoarding in non-serotonergic cells has not yet been determined. The explanation may be as simple as a mechanism for clearing excess 5-HT out of the extracellular space. Another possible explanation is that these neurons use the collected 5-HT for transmitting purposes.

3. 5-HT_{2A} receptor

Pharmacologically, 5-HT regulates SA in the hindbrain (Hunt et al., 2005). In order for this to be possible, 5-HT must be activating receptors expressed in hindbrain cells during the window of SA. There are 7 classes of 5-HT receptors that are primarily G-protein coupled receptors (GPCRs), with a total of 15 known subtypes (Guiard & Di Giovanni, 2015). Only one ionotropic receptor has been identified, 5-HT_3. This dissertation will focus on the 5-HT_2 family of receptors, as the general antagonist of this family, ketanserin, blocks hindbrain SA (Hunt et al., 2006; Hunt et al., 2005).

There are 3 members of the 5-HT_2 family of receptors: 5-$HT_{2A,}$ 5-HT_{2B}, and 5-HT_{2C}. All 3 GPCRs couple to G_q, an excitatory G protein that canonically increases levels of intracellular calcium from internal stores. Ketanserin has the highest affinities for the 5-HT_{2A} and 5-HT_{2C} receptors, with a K_i of 2-3 nM and 130 nM, respectively. However, at the high concentrations used in our experiments (10μM), Ketanserin also possesses an affinity for a multitude of other receptors and systems including 5-HT_{2B} receptor, histamine receptors, dopamine receptors 1 and 2 (D1 and D2), norepinephrine receptors and VMAT2 (Hunt et al., 2005; Shih et al., 1999). Many of these other proteins are expressed in the early hindbrain and represent potential confounds in

our central hypothesis that 5-HT initiates hindbrain SA. VMAT2, for example, would also be needed for 5-HT to be packed into vesicles and released for signaling. More selective antagonists exist that reduce the risk of nonspecific side effects. A potent and selective antagonist for the 5-HT_{2A} receptor (5-HT_{2A}R), the most relevant subtype based on our data, is M100907 (Kehne et al., 1996).

5-HT_{2A}R is widely expressed in neurons and glia throughout the central and peripheral nervous systems (Wirth, Holst, & Ponimaskin, 2016). In the adult mouse CNS, the densest expression has been found throughout the forebrain via immunostaining, autoradiographic approaches, *in situ* hybridization (ISH), and transgenic reporters. Specifically, pyramidal cells in the anterior cerebral cortex, a subpopulation of GABAergic cortical interneurons, and non-pyramidal cortical neurons in layer VIb express 5-HT_{2A}R (Weber & Andrade, 2010). The amygdala, ventral striatum and hippocampus are also rich in 5-HT_{2A}R (Weisstaub, 2006). In the hindbrain, both immunostaining and ISH have shown embryonic expression of 5-HT_{2A}R (Hunt et al., 2005). The Allen developing mouse brain atlas detects mRNA for 5-HT_{2A}R in the hindbrain, lateral to the ventral midline on both sides, at the stage of SA onset (Figure 7) (http://developingmouse.brain-map.org/).

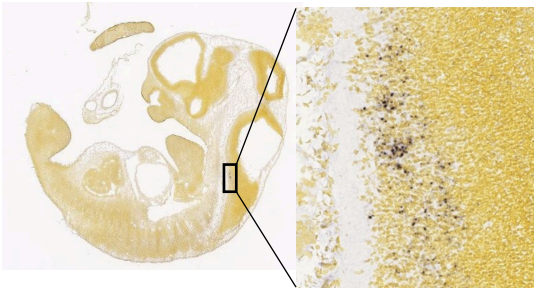

Figure 7: ISH of htr2a gene in E11.5 mouse. Sagittal section through E11.5 mouse embryo showing mRNA (dark spots) for 5-HT_{2A}R is expressed in ventral hindbrain. (Allen brain atlas)

5-HT_{2A}R forms stable homo-and heterodimers with other GPCRs like metabotropic glutamate receptor 2 (mGluR2) and D2. The functional significance of these complexes is largely undetermined, but likely contributes to differences in binding properties for various ligands

(Guiard & Di Giovanni, 2015). Depending on the ligand, 5-HT_{2A}R has the ability to recruit the signaling protein β-arrestin2, which is believed to regulate intracellular trafficking of 5-HT_{2A}Rs (Guiard & Di Giovanni, 2015). Activation of 5-HT_{2A}R reportedly modulates dopamine transmission within the limbic system, as well as increases glutamate transmission in the prefrontal cortex and nucleus accumbens (Barr et al., 2004; Wirth et al., 2016). Dysfunctional 5-HT_{2A}R signaling is also implicated in the etiology of schizophrenia, sleep disorders and mood disorders like depression and anxiety (Wirth et al., 2016).

Hallucinogenic compounds, like psilocybin and lysergic acid diethylamide (LSD), are potent agonists of 5-HT_{2A}R. 5-HT_{2A}R antagonists block the psychoactive effects of hallucinogens in animals including mice, rats and humans, supporting a primary role for these receptors in inducing the behavioral and cognitive changes associated with drug intake (Gonzalez-Maseo et al., 2007). Not all 5-HT_{2A}R agonists are hallucinogenic; for example, endogenous 5-HT and agonists like 1-(2,5-dimethoxy-4-iodophenyl)-2-aminopropane (DOI) do not elicit hallucinogenic activity (González-Maeso et al., 2007). However, these agonists also activate other 5-HT receptors. The diverse mechanisms, networks and signaling cascades leading to the dichotomy of responses to 5-HT_{2A}R agonists remains unclear.

5-HT_{2A}R knockout mice have been generated and analyzed for both CNS and intestinal abnormalities, as the receptor is abundant throughout the brain and enteric nervous system (Fiorica-Howells, Hen, Gingrich, Li, & Gershon, 2002). In the brain, no morphological aberrations or changes in cytoarchitecture have been detected (Weisstaub, 2006). The mice reach maturity with no blatant health handicaps, although the mice are more prone to seizures and exhibit deficits in fear and anxiety behaviors (Guiard & Di Giovanni, 2015; Weisstaub, 2006).

Unfortunately, no studies have examined spontaneous activity during the development of 5-HT_{2A}R knockouts.

Some of the morphogenic functions of 5-HT in development are mediated through the 5-HT_{2A}R. For example, application of the 5-HT_{2A}R agonist DOI upregulates brain-derived neurotrophic factor (BDNF) mRNA levels (Vaidya, Marek, Aghajanian, & Duman, 1997). This is one way that 5-HT signaling supports cell survival, due to the trophic support provided by BDNF for the survival and morphogenesis of CNS neurons (Numakawa et al., 2010; Rios et al., 2006). Conversely, there is also a significant reduction of 5-HT_{2A}R expression in mice lacking BDNF postnatally, despite an otherwise intact and functional serotonergic system (Rios et al., 2006). This suggests BDNF and5-HT_{2A}R regulate each other.

Cell proliferation during adult neurogenesis can also be modulated by the elimination of 5-HT_{2A}R signaling (Wirth, 2016). However, the length of time over which signaling is disrupted determines the direction of modulation. The number of progenitors proliferating in the subgranular layer of the adult rat dentate gyrus decreased in response to one treatment of ketanserin to block 5-HT_{2A}R signals (Banasr et al., 2004). A similar decrease was found in rats following a single treatment of ketanserin by Jha et al., however found an opposite effect was found when administering chronic treatment for 7 consecutive days (2008). The long-term elimination of 5-HT_{2A}R signals resulted in a 46% increase in the proliferation of hippocampal progenitor cells.

Current project

Cells in the early embryonic mouse hindbrain depolarize without external stimulation. This depolarization is termed spontaneous activity (SA) and triggers intracellular calcium influx. The activity begins as isolated events at embryonic day (E) 10.5 and shifts into synchronized waves

across hindbrain neurons by E11.5. These waves propagate along the ventral floorplate of the neural tube. The exact function of this activity is unknown.

During this same developmental window, all of the brain's serotonergic neurons are born in the hindbrain adjacent to the spontaneously active midline. Pharmacological studies have previously implicated the involvement of serotonin, also called 5-hydroxytryptamine or 5-HT, in the initiation of spontaneous events (Hunt et al., 2006; Hunt, McCabe, et al., 2005). However, the antagonist utilized in these studies possessed documented affinities for other relevant molecules expressed early in the hindbrain (i.e. vesicular monoamine transporter 2 (VMAT2), other monoamine neurotransmitters). The present study employed highly selective antagonists with less potential for nonspecific effects to further probe the relationship between serotonergic signaling and spontaneous activity. The data support the hypothesis of 5-HT's central role in event initiation.

Further, early embryonic hindbrains were subjected to 24 hours of SA interruption *in vitro* in attempt to determine a functional role for activity in hindbrain development. We first examined the effect of eliminating waves and 5-HT signaling on the cells that help initiate them, the serotonergic neurons. Hindbrains cultured in selective serotonin antagonists during the period of serotonin neurogenesis show a significant reduction in the number of 5-HT+ neurons that develop. The remainder of this dissertation investigates broad explanations of why the cell reduction occurs.

4. Materials and methods

The majority of this research was conducted at the University of Washington in Seattle, as part of Dr. Martha Bosma's lab. Some immunohistochemistry was completed at Arizona State University in Tempe, Arizona in Dr. Michael Foster Olive's lab. Any differences in equipment and protocols used between the two locations will be noted.

Animals

Experiments at the University of Washington were completed with Swiss Webster mice housed in a 12:12 light cycle, with food and water available ad libitum. One exception was the transgenic line used in Fig3. This transgenic line was the product of a Pet1-cre mouse crossed with a floxed tdTomato reporter mouse, with C57/Bl6 as the background strain, to specifically label the Pet1+ subpopulation of 5-HT neurons. C57/Bl6 mice were used at Arizona State University, housed in a 10:14 reverse light cycle. No physiological differences have been detected in SA between strains (Gust, Wright, Pratt, & Bosma, 2003). For all experiments, mice were mated and monitored for vaginal sperm plugs in order to gauge the start of pregnancy. Mothers were sacrificed via CO_2 asphyxiation and cervical dislocation, in accordance with the IACUC of both universities, 10 or 11 days post-plug observation to harvest embryos depending on the experiment. Theiler criteria was used to verify the developmental stage for each individual embryo. Theiler staging is more precise than relying solely on plug times (Gust et al., 2003).

Hindbrain dissection

Hindbrains were isolated and dissected into an open-book conformation, in which the neural tube was opened at the dorsal roof plate and laid flat on the ventral surface, with the exposed dorsal surface, or ventricular layer, facing upwards. The dissection procedure, detailed in Figure 8, was performed with ultra fine-tip forceps and magnified 30x under a Zeiss dissection microscope. The hindbrains were dissected in artificial cerebral spinal fluid (ACSF) containing (in mM): NaCl, 119; KCl, 2.5; $MgCl_2$, 1.3; $CaCl_2$, 2.5; NaH_2PO_4, 1; NaHCO3, 26; glucose, 30; oxygenated with carbogen (95% O_2, 5% CO_2). As much non-neural tissue was removed from the ventral surface as possible without damaging the underlying hindbrain. This is difficult to achieve as layers of tissue are more difficult to separate at early embryonic stages compared to E12.5 and older; torn hindbrains were excluded from experiments.

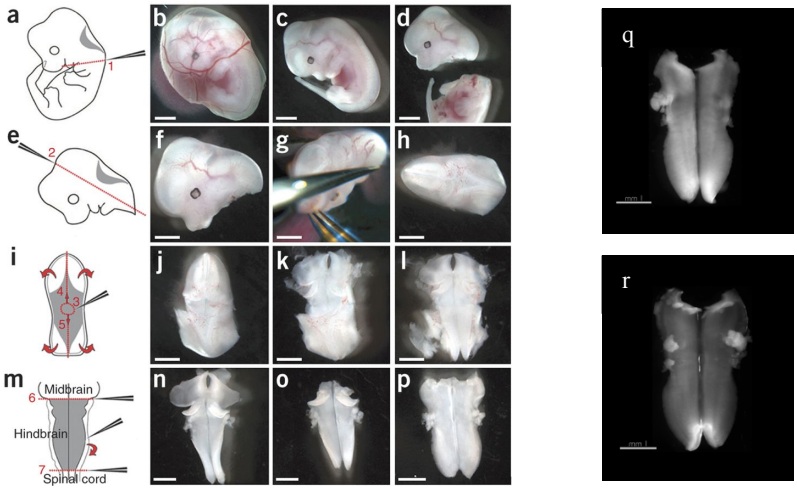

Figure 8: Example of an E12.5 hindbrain dissection for open-book preparation (p). The body is removed anterior to the forelimb (a,d), followed by removal of the face and forebrain (e,g). Lastly, the dorsal roof plate is cut open (i-k). (q) displays the dorsal surface of an isolated E11.5 hindbrain, which is the ventricular layer that previously lined the neural tube. (r) displays the ventral surface of an isolated E11.5 hindbrain that has been cleared of somatic tissue. (Fantin et al. 2013; Hiro Watari)

Culture paradigm

All harvested embryos were dissected before placement on Millipore culture inserts with 0.4µm pore size beneath a dissection microscope, with isolated hindbrains incubating at room temperature in carbogen-saturated ACSF until all specimens were ready for plating. Two hindbrains were

allotted to each culture insert. The inserts were then transferred to Falcon 35x10 petri dishes filled with 1 mL each of culture media containing the following: sterile 75% Neurobasal-A medium (1x); 25% horse serum; 2 mM L-glutamine; 100 IU/mL penicillin; 0.1mg/mL streptomycin. Cultures were incubated for 24 hours at 37º C with a 5% CO_2 environment in a Thermo-Scientific Model 3100 water jacket incubator. Each control was size-matched to each drug-treated pair.

Pharmacology

Pharmacological agents were added to culture media for 24-hour exposure in culture or ASCSF for Ca^{2+} imaging experiments. All reagents were dissolved in dimethyl sulfoxide (DMSO) and used at the following concentrations (in μM): Ketanserin,10; M100907, 50; Mibefradil, 10. Control culture medium was supplemented with DMSO in equal volume. For Ca^{2+} imaging experiments, drugs were added to ACSF. The antagonists for 5-HT receptors used in Ca^{2+} imaging are listed below:

Ketanserin: Ki= 4 nM for 5-HT_{2A}R and 120 nM for 5-HT_{2C}R (Kasper, Booth, & Peris, 2015).

M100907: Ki=0.85 nM for 5-HT_{2A}R (Kehne et al., 1996).

SB242084: Ki=2.1 nM 5-HT_{2C}R (Ward, Pediani, Godin, & Milligan, 2015).

RS 102221: Ki=16.6 nM 5-HT_{2C}R (Ward et al., 2015).

Zacopride Hydrochloride: Ki = 0.32 nM (Donahue et al., 2017).

Ca^{2+} imaging

The experiments were completed with Chris Vong. Cultured hindbrains, or freshly isolated hindbrains (acute) in the open-book conformation, were incubated for 15 minutes in a continuously-oxygenated solution of ACSF, the fluorescent calcium-binding dye Fluo-8, and the permeabilization detergent pluronic F-127 at room temperature. After washes in ACSF, brains were placed in a clear imaging chamber, dorsal-surface down (Fig 6q), and held in place with a

harp. The chamber was continuously perfused with oxygenated ACSF at a flow rate of 1-2 mL/minute. Brains were allowed to stabilize in perfusion environment for 10 minutes before imaging. Changes in fluorescence were measured in 48 regions of interest created across the hindbrain using MetaFluor. Images were collected at 10x magnification on an inverted flurescent microscope, captured at a rate of 1Hz. At least 10 minutes of baseline activity was recorded in each experiment before bath application of any pharmacological drugs. Experiments were completed at 25 º C.

Immunohistochemistry (IHC) for Cryosections

Cultures were fixed with 4% paraformaldehyde (PFA) for 30 minutes at room temperature and cryoprotected in 30% sucrose overnight at 4 ºC. The brains were transferred into Sakura 10x10x5mm cryomolds filled with OCT compound and flash frozen on dry ice. Transverse sections ranging from 30-40 μM in thickness were collected directly onto coated slides using a Leica cryostat. At the University of Washington, slides coated with Vectabond were used, while at Arizona State University, slides were coated with gelatin. Both adhesion methods were equally successful in securing tissue sections to Fisher superfrost slides after heating for one hour at 55ºC on a Fisher Scientific slide warmer. Prior to heating the slides, a hydrophobic barrier was drawn onto each slide surrounding the tissue sections using an ImmEdge pen.

After heat treatment, all slides immediately began a series of three 10-min washes with gentle agitation on an orbital shaker in PBS-T, a phosphate-buffered saline solution containing 0.1% Triton X-100. All washes and solutions were applied directly onto the slides, corralled by the hydrophobic barrier. Tissue sections were blocked from nonspecific staining with a one-hour incubation in 5% normal donkey serum in PBS-T on an orbital shaker at room temperature. A complete list of antibodies and concentrations used in PBS-T is supplied in Table 1. 5-HT primary

antibodies were incubated for 3 nights at 4 ºC while shaking, while all remaining antibodies incubated for 1 night. Next, slides received three 10-min washes with PBS, followed by a 2 hour incubation in secondary antibody. Three 10-min PBS washes followed, with a final fourth wash of distilled water to rinse off any lingering salts. In the Bosma lab, an additional step for DAPI (1:1000) application, to label all cell nuclei, was included for 5 min prior to the final PBS washes. In the Olive lab, the mounting medium (Vectashield) contained DAPI and no additional application step was needed. The Bosma lab used Fluoromount mounting media, and both labs utilized 22x50mm Fisherbrand microscope cover glass. The mounting medium was allowed to set overnight, and then the edges of the cover glass were sealed with clear nail polish.

Passive Clarity Technique (PACT):

Wholemount images were obtained from transparent hindbrains that had been cleared of all lipids through PACT as described by Yang et al., omitting only nitrogen degassing (2014). Hindbrains were isolated and dissected into an open-book conformation as described above, then fixed in 4% PFA for 30 minutes. The tissue was then incubated at 4 °C overnight in a solution containing the hydrogel monomer solution A4P0 (4% acrylamide in PBS) supplemented with 0.25% photoinitiator 2,20 -Azobis[2-(2-imidazolin-2-yl) propane]dihydrochloride (VA-044, Wako Chemicals USA) (Yang et al. 2014). The excess hydrogel was removed during three PBS washes, followed by gentle agitation in 0.1M PBS with 8% SDS (pH 7.5) for 2-5 days at 37°C.

For immunostaining, the samples were first washed five times in PBS over the course of one day. Primary antibodies were applied at 1:200 in PBS containing 2% normal donkey serum, 0.1% Triton X-100 and 0.01% sodium azide for 3–7 days. Brains were washed for one day in PBS and then incubated in secondary antibodies at 1:300 for 2–5 days. After one final day of PBS washes, the brains incubated in RIMS imaging media comprised of: 40 grams of Histodenz, 30

ml of 0.02 M PB, 0.1% tween-20 and 0.01% sodium azide. pH 7.5 with NaOH. Incubation continued until brains were transparent, around one day, and then were mounted on a glass slide with RIMS.

Confocal Microscopy and Cell counting:

All presented images were collected on a Leica SP5 confocal. Every image was captured in a z-stack with dual channels (i.e. DAPI and protein of interest). All 5-HT+ cells per brain were manually counted using the manual cell counter plug-in in ImageJ. At least two people counted every image and the numbers averaged. The nuclear stain of Isl1/2+ cells allowed for ImageJ to semi-automate the counting process. Particles were measured after manually thresholding each image, applying a 0.2 watershed and setting the size threshold from 9-infinity to obtain the cell numbers. The accuracy of these thresholding and watershed features in the semi-automated counting was verified with manual counts in ImageJ using the manual cell counter plug-in.

III. Results

5-HT_{2A} signaling regulates SA.

We first tested the hypothesis that active 5-HT_2 receptors are necessary for the production of SA in the hindbrain. Ca^{2+} imaging experiments were conducted on acute E11.5 hindbrains using selective antagonists for 3 different 5-HT receptors. 5-HT_{2A} and 5-HT_{2C} receptors were selected to verify previously published data that utilized Ketanserin at concentrations with potential off-target effects. We also tested for the involvement of the 5-HT_3 receptor; its permeability to Na^+, K^+ and Ca^{2+} made this subtype an appealing candidate for influencing cell excitability.

At all concentrations tested, the 5-HT_{2C}R antagonists did not significantly decrease the frequency of spontaneous events. The average frequency of events before SB24084 application

was 3.55±1.05 events/min, while the average frequency of events after application of the highest dose tested (100 μM) was 2.25±0.86 events/min (Figure 9A). This difference was not significant (paired t-test, p= 0.18). The average frequency of events before RS 102221 application was 4±0.48 events/min, while the average frequency of events after application of the highest doses tested (100 and 150 μM) was 3±0.55 events/min (Figure 9B). This difference was not significant (paired t-test, p= 0.27). The failure of both drugs to fully reproduce the effects of Ketanserin suggests the 5-HT_{2C} receptor subtype is not the primary 5-HT receptor involved in hindbrain SA.

Blockade of the 5-HT_3 receptor significantly reduced the frequency of SA (Figure 9C). The average frequency before Zacopride hydrochloride application was 4.86±0.51 events/min, while the average frequency after application of an 80 μM dose was 3.46±0.75 events/min (paired t-test, p=0.030). However, this antagonist did not consistently stop all spontaneous calcium events, as Ketanserin does, even at the 100 μM dose (Hunt et al., 2006). The only receptor subtype tested that fully recapitulated the effects of Ketanserin was the 5-HT_{2A}R (Figure 9D). The average frequency of events before M100907 application was 2.8±0.25 events/min, and the frequency of events in every experiment after application of 50 μM M100907 was 0 (paired t-test, $p<0.001$). A minimum dose of 50 μM was required to fully stop all spontaneous events, and thus this dose was used for subsequent culture experiments. SA also returned after washing with normal ASCF.

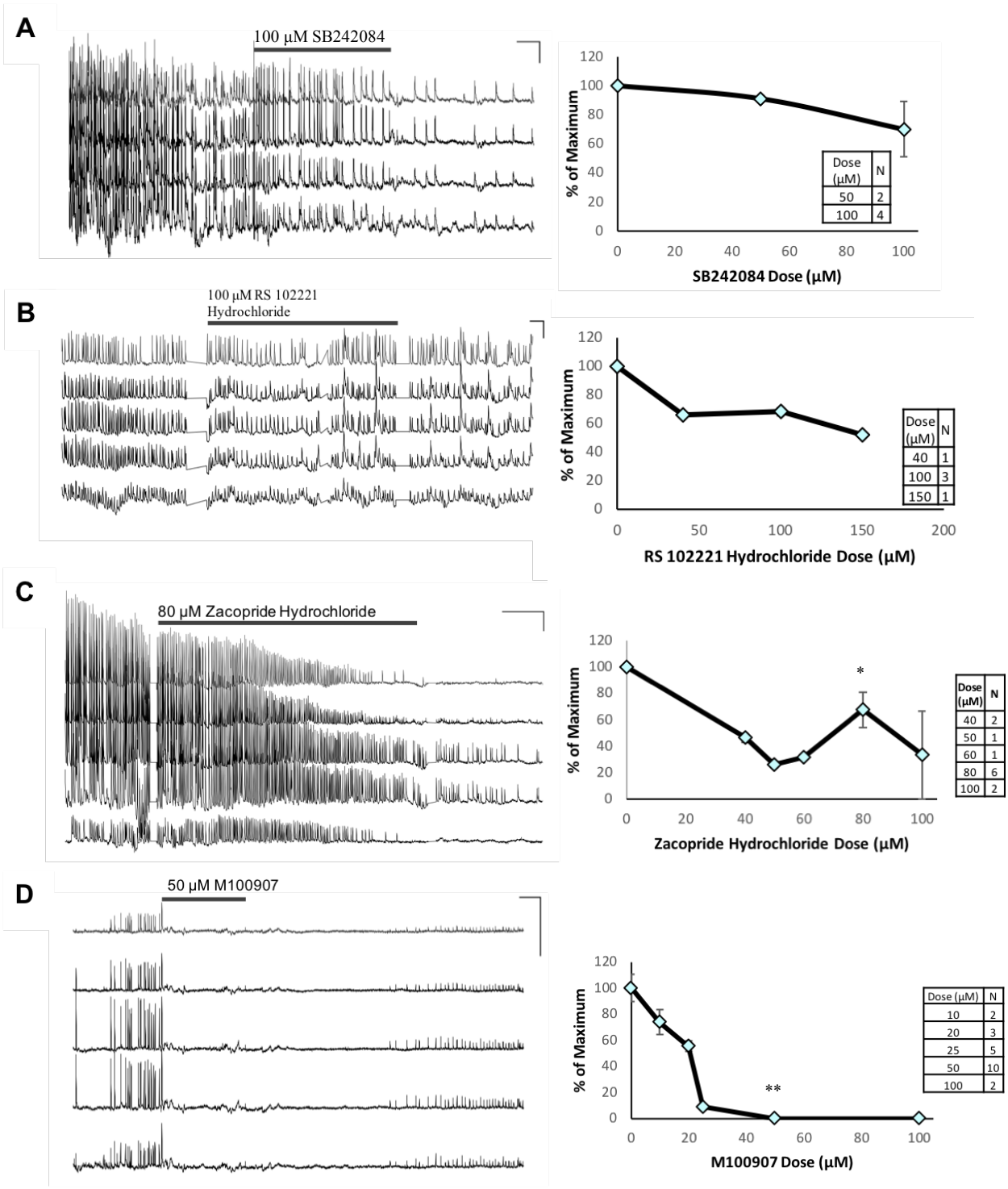
A
100 µM SB242084
% of Maximum
SB242084 Dose (µM)
Dose (µM) N
50 2
100 4
B
100 µM RS 102221 Hydrochloride
% of Maximum
RS 102221 Hydrochloride Dose (µM)
Dose (µM) N
40 1
100 3
150 1
C
80 µM Zacopride Hydrochloride
% of Maximum
Zacopride Hydrochloride Dose (µM)
*
Dose (µM) N
40 2
50 1
60 1
80 6
100 2
D
50 µM M100907
% of Maximum
M100907 Dose (µM)
**
Dose (µM) N
10 2
20 3
25 5
50 10
100 2

Figure 9: Acute treatment with M100907 stops SA. Each row features representative Ca^{2+} traces from hindbrains treated with 5-HT antagonists (left). The drug application period is denoted by grey bar above the trace. The dose response curve for each drug is on the right. *p<0.05, **p<0.001 Scale= 5 ΔF/F, 5 min **(A)** 5-HT_{2C}R antagonist SB242084 **(B)** 5-HT_{2C}R antagonist RS 102221 Hydrochloride **(C)** 5-HT_3R antagonist Zacopride Hydrochloride **(D)** 5-HT_{2A}R antagonist M100907. Error bars= SEM. If N>3 and error bar is not visible, then SEM is smaller than data marker.

We next tested the hypothesis that deficits in SA became permanent after longer-term M100907 treatment. Hindbrains were exposed to M100907 for 24 hours in culture and then Ca^{2+} imaged in normal ACSF (Figure 10). The average frequency of SA in hindbrains that had been cultured in M100907 is 1.9±0.48 events/min. This is not significantly different than the average frequency of control cultures, 1.6±0.40 events/min (2 sample t-test, p=0.6652).

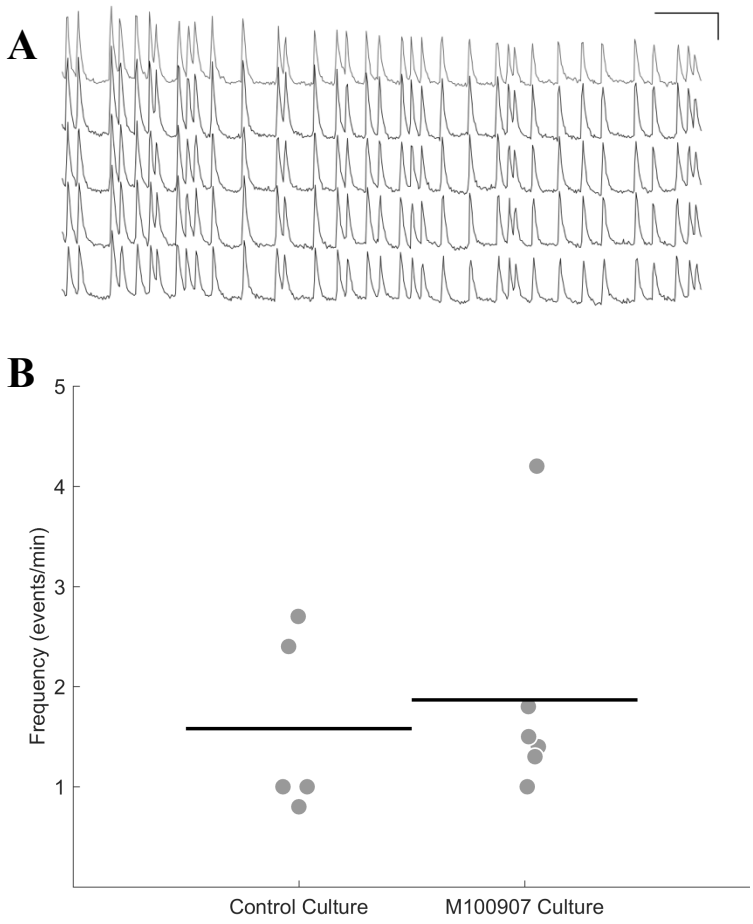

Figure 10: Hindbrains with chronic M100907 treatment maintain ability to produce SA. (A) Representative Ca^{2+} trace of M100907 culture. Scale= 5 ΔF/F, 1 min. **(B)** The frequency of SA for control (N=5) and M100907 cultures (N=6). Black bar = average frequency.

Culture protocol is sufficient model for hindbrain development.

The culture paradigm used has never been published and required validation. We first evalaued SA in hindbrains cultured for 24 hours. There are no spontaneous waves of activity in acute E10.5 hindbrains (Figure 11C). Twenty-four hours later, at E11.5, acute hindbrains experience an average of 2.5±0.35 events/min. Hindbrains that are harvested at E10.5, before SA is present, and cultured one day *in vitro* (DIV) develop waves of midline activity as would be expected in natural

development, albeit at a slower average frequency of 1.6±0.40 events/min (Figure 11B, C). This frequencies of acute E11.5 and cultured hindbrains are not significantly different (2 sample t-test, p=0.0844). The frequency of cultured hindbrains is significantly differnet from acute E10.5 hindbrains (2 sample t-test, p=0.0279).

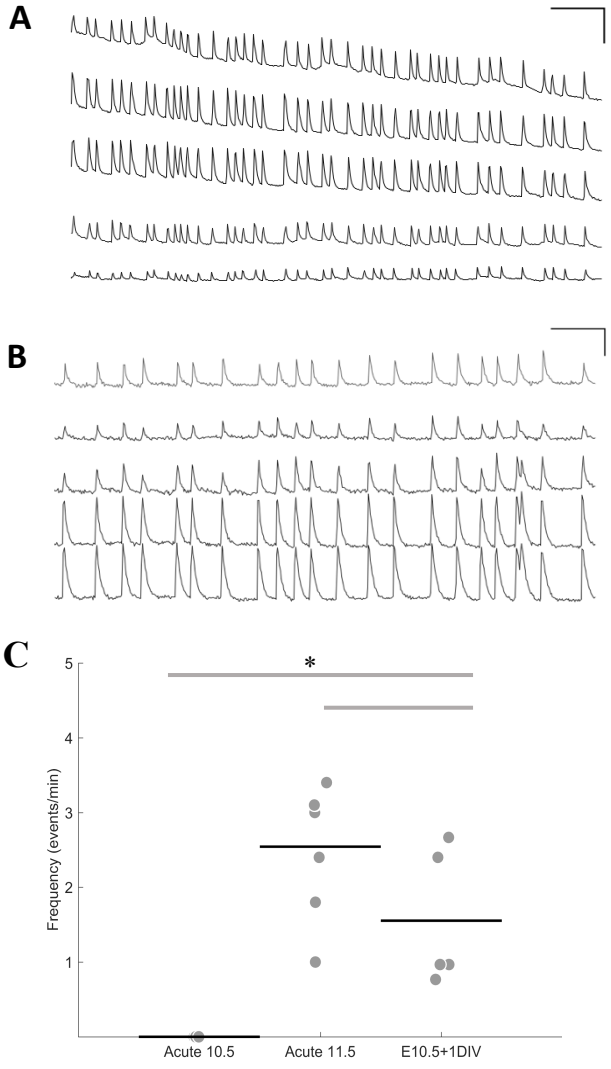

Figure 11. Cultured hindbrains develop waves of SA. **(A)** Representative Ca^{2+} imaging trace from an acute E11.5 hindbrain. **(B)** Representative Ca^{2+} imaging trace from an E10.5 + 1 DIV hindbrain. Scale= 5 ΔF/F, 1 min. **(C)** Average frequency of spontaneous events over a 30 minute

interval for acute E10.5 (N=3), acute E11.5 (N=7) and E10.5 +1DIV control (N=5) hindbrains. Black bar = average frequency. *p<0.05.

Cultured hindbrains were then analzyed for 5-HT+ cell numbers (Figure 12). 5-HT is not detectable in E10.5 hindbrains. By the next developmental stage, E11.5, abundant 5- HT is expressed in cells throughout the p3 domain of the rostral hindbrain, with an averge of 971±165.6 cells. After a 24-hour culture period, 5-HT+ cells are also detectable in the cultured brains, with an average of 594±82.3 cells. The average number of 5-HT+ cells produced in culture is lower than in acute E11.5 brains, but not significantly different (2 sample t-test, p=0.1109). The number of 5-HT+ cells in culture is significantly differnet from the number of 5-HT+ cells at E10.5 (2 sample t-test, p=0.0015). These data support the culture paradigm as an appropriate model for hindbrain development, due to the prescence of SA and 5-HT neurogenesis in both acute E11.5 brains and cultured E10.5 + 1DIV brains.

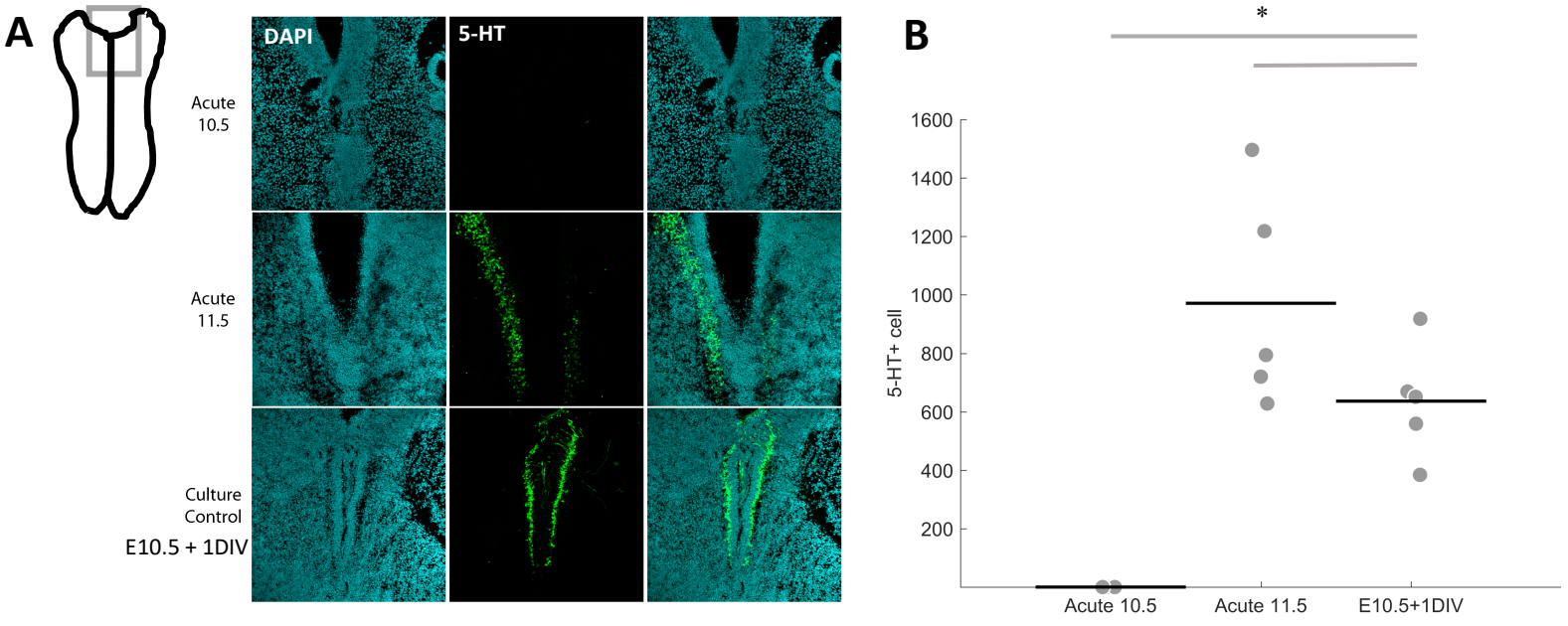

Figure 12: 5-HT+ cells develop in culture. **(A)** Immunostain of 5-HT (green) across 2 developmental stages compared to E10.5 + 1DIV culture (bottom row). Nuclei labled with DAPI (cyan). Location in hindbrain denoted to the left by grey box **(B)** Quantification of 5-HT+ cells for acute 10.5 (N=3), acute E11.5 (N=5) and E10.5+1DIV (N=6) hindbrains. Black bar = average 5-HT+ cells. *p<0.05.

5-HT$_{2A}$ signaling regulates number of 5-HT neurons

Hindbrains were cultured in 5-HT$_{2A}$R antagonists for 24 hours to evaluate the effects of long- term treatment on hindbrain development. We hypothesized extended exposure would disrupt normal hindbrain development. The serotonin population was analyzed for changes in cell number.

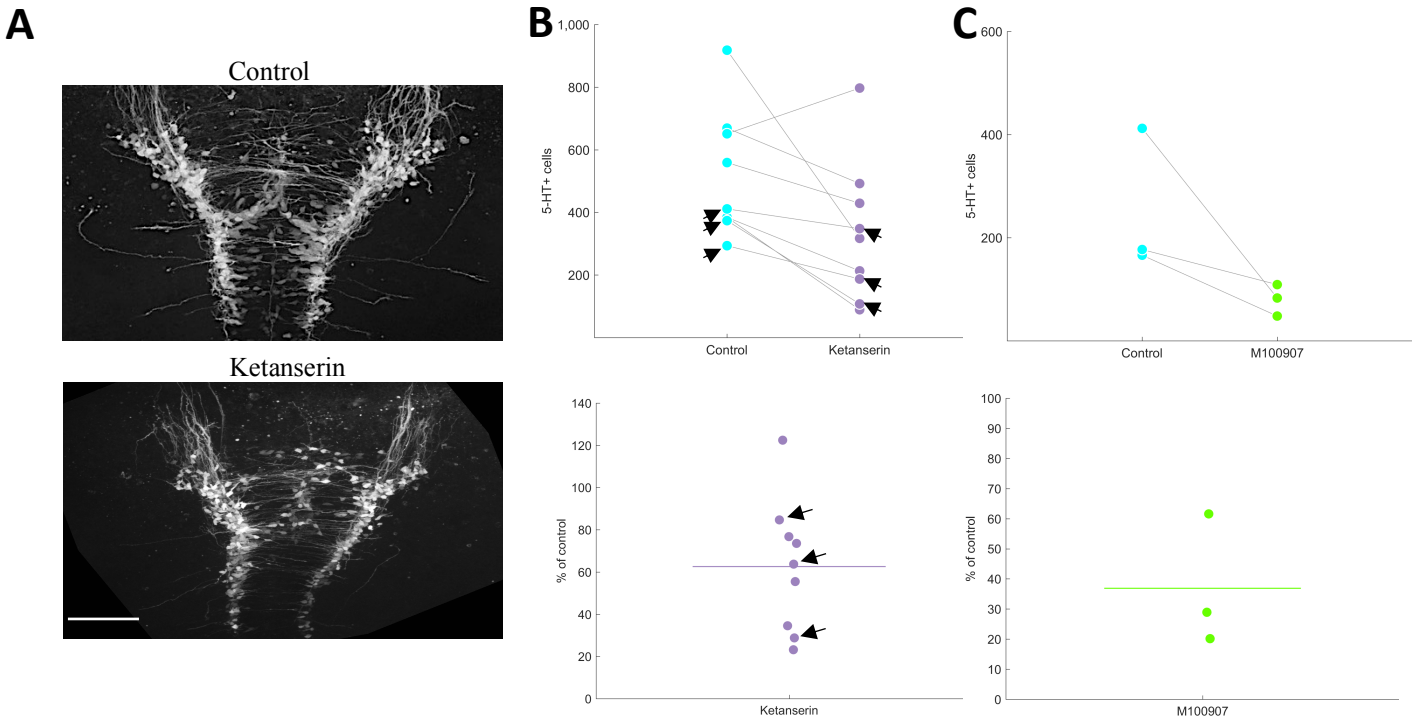

Figure 13: Number of 5-HT+ cells is reduced after 24 hours of disrupted 5-HT$_{2A}$ signaling. **(A)** Rostral 5-HT+ cells in whole mount cultures cleared via PACT. **(B)** Quantification of rostral

5-HT+ cells, in both sliced and whole mount preparations of E10.5 + 1DIV hindbrains (top). Arrows indicate whole mount preparations. Cell numbers in Ketanserin cultures are on average 62.6% of paired control cell numbers (bottom) **(C)** Rostral 5-HT+ cells in E10.5 +1DIV hindbrains cultured with the selective 5-HT_{2A}R antagonist M100907 (50 μM) and control cultures (top). 5-HT+ cell numbers in M100907 cultures are on average 36.8% of paired control cell numbers (bottom).

During the culture period (E10.5+1DIV), 50% of the rostral 5-HT neurons are generated, and no caudal 5-HT neurons are generated yet. Hindbrains cultured in Ketanserin had an average of 331.1±74.2 5-HT+ cells (Figure 13B, top). This is significantly fewer 5-HT+ cells compared to paired control cultures, which had an average of 515.9±66.7 (paired t-test, p=0.0251). On average, the 5-HT+ cell numbers in Ketanserin cultures were reduced by 37.4% compared to control cell numbers (Figure 13B, bottom). The 9 culture pairs used were from 4 different litters of animals. The pairs within litters were assigned by matching embryos of equivalent size. The hindbrains analyzed as whole mounts are denoted by arrows (Figure 13B). The 3 pairs denoted by arrows are the only whole mounts presented in this dissertation; every other hindbrain was cryosectioned. It is important to note there are 2 waves of rostral 5-HT neurogenesis. 50% of rostral 5-HT cells are born in r1 from E9.5-10.5 and the remainder in r2-3 from E10.5-11.5. By the time the E10.5 cultures begin, 50% of rostral 5-HT neurons have already been generated in r1. The E10.5+1DIV cultures target the second wave of 5-HT neurogenesis, and a 37.4% reduction represents a large proportion of the total 5-HT+ cells generated during this window.

When assessed using the selective 5-HT_{2A}R antagonist M100907 (Figure 13C), the average 5-HT+ cells in control cultures was 251.7±80.2 and the average number was 80±17.7 in M100907 cultures (paired t-test, p=0.16).

The cell reduction in the rostral population of 5-HT+ cells only occurred when hindbrains were cultured during the window of rostral 5-HT neurogenesis (Figure 14). E11.5-12.5 marks the onset of caudal 5-HT neurogenesis. Control hindbrains cultured from E11.5 to E12.5, after rostral neurogenesis is complete in r1-3, had an average of 527±38.2 rostral 5-HT+ cells. The average number of rostral 5-HT+ cells in Ketanserin cultures was 522±60.1 (paired t-test, p=0.96). Each pair is from a different litter of animals. In the caudal 5-HT+ cell population of these cultures, there was an average of 685±313.9 5-HT+ cells for controls and 439.7±184.7 5-HT+ cells for Ketanserin cultures (paired t-test, p=0.26).

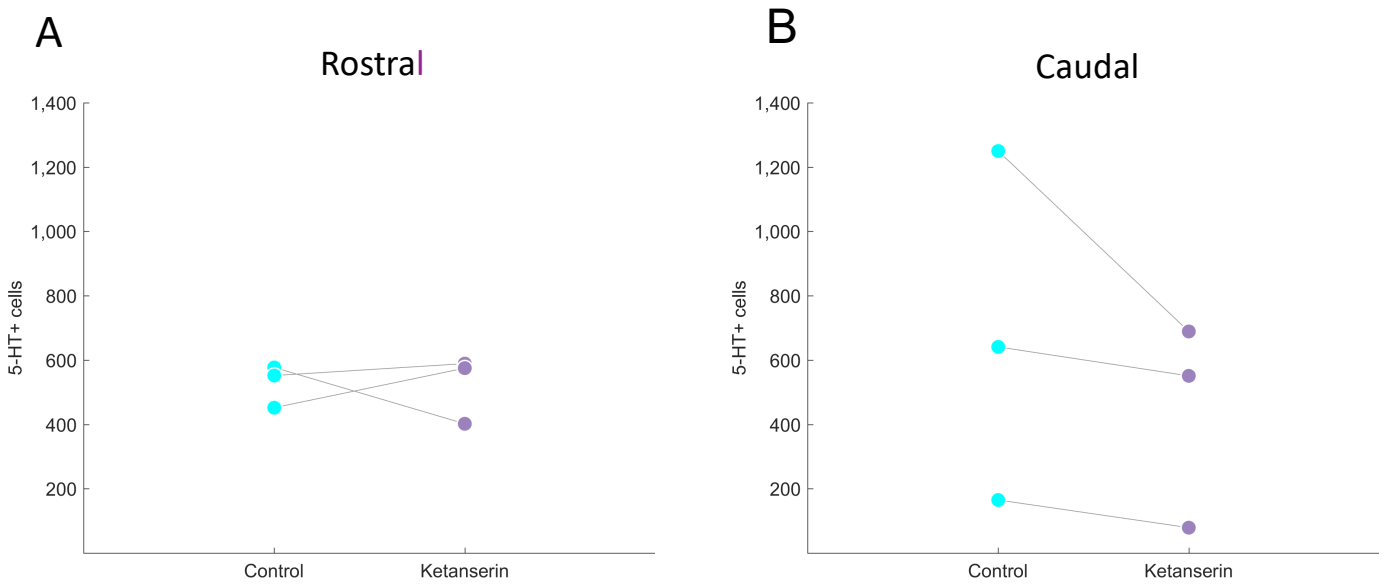

Figure 14: Reduction in rostral 5-HT+ cells only occurs during window of rostral 5-HT neurogenesis. (A) Quantification of rostral 5-HT+ cells in 3 pairs of sliced E11.5 +1DIV

hindbrains. Control cultures are shown in cyan and Ketanserin (10 µM) cultures are shown in purple. **(B)** Quantification of caudal 5-HT+ cells in the same pairs of E11.5 +1DIV hindbrains. Control cultures are shown in cyan and Ketanserin (10 µM) cultures are shown in purple.

Our next aim was to determine whether the 5-HT+ cell reduction was a result of disrupted SA or a result of disrupted 5-HT_{2A}R signaling. This was tested by stopping SA independently of 5-HT_{2A}R signaling and assessing the number of 5-HT+ cells (Figure 15, left). The Bosma lab has already established the T-type Ca^{2+} channel antagonist Mibefradil fully blocks spontaneous calcium events (Moruzzi et al., 2009). When cultured in Mibefradil, cultures developed an average of 545±1007.2 5-HT+ cells. This is not significantly different from the average control number of 5-HT+ cells, which was 564± 130.6 (p=0.66). The Mibefradil cultures exhibited, on average, 105% of the 5-HT+ numbers in paired controls (Figure 15, right). This data suggests the cell reduction observed after treatment with 5-HT_{2A} antagonists is not dependent on SA.

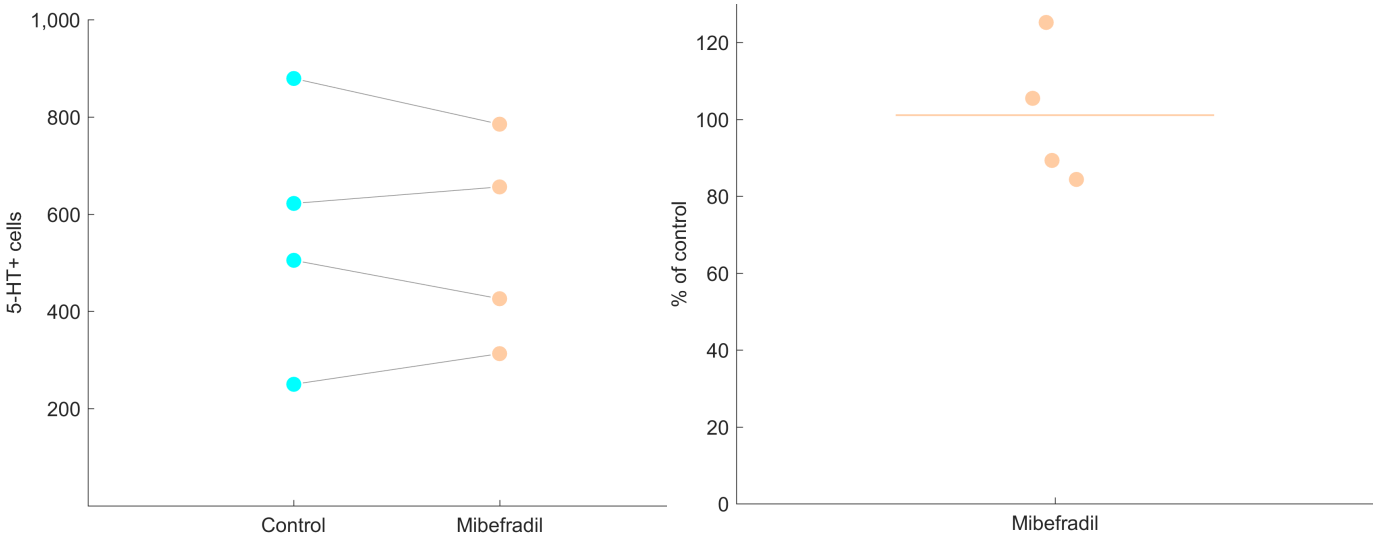

Figure 15: 5-HT+ cell reduction is not activity dependent. Quantification of 5-HT+ cells in 4 pairs of sliced E10.5 + 1DIV hindbrains (left). Control hindbrains are shown in cyan and Mibefradil-treated (10μM) hindbrains are shown in peach. The number of 5-HT+ cells in Mibefradil cultures is on average 105% of the 5-HT+ cell numbers in paired control cultures (right). Average shown by horizontal line.

We next aimed to determine if other cell populations were affected by disrupted 5-HT_{2A} signaling, or if the cell number reduction is specific to the 5-HT lineage (Figure 16). The other population of neurons made from p3 progenitors around this same time frame were the ideal candidate, the visceral motor neurons (VMN). r4-7 are still producing VMNs during the culture period. When p3 progenitors are prevented from specifying the 5-HT lineage in the $Foxa2^{-/-}$ mouse, the progenitors instead make extra VMNs (Jacob et al., 2007). This is not the case in our cultures. The mean number of Isl1/2+ cells in control cultures was 17,801.2±2,742.2. This was not significantly different from the mean number of Isl1/2+ cells in M100907 cultures, 14,855.7±2,581.6 (paired t-test, p=0.34). The data support a 5-HT specific effect of cell number regulation through 5-HT_{2A} signaling.

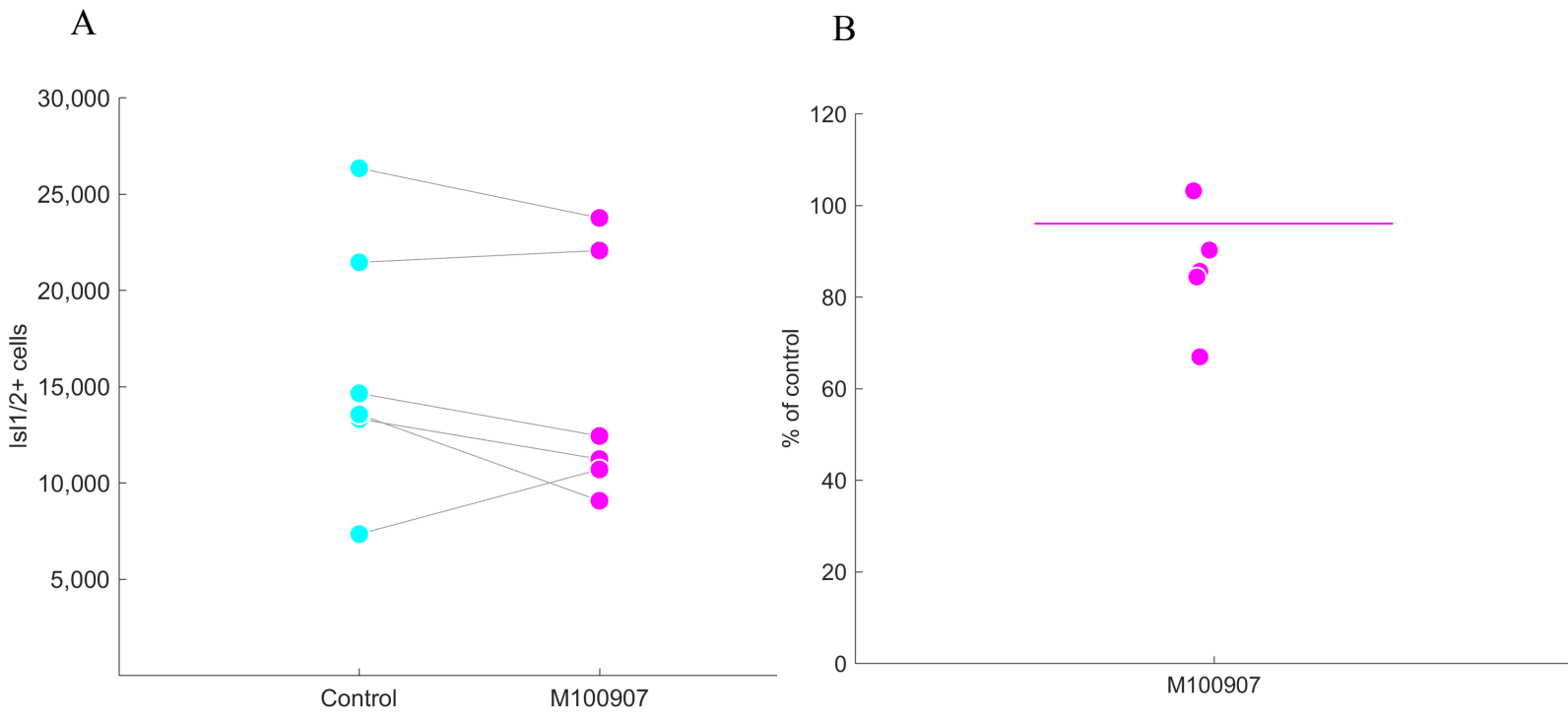

Figure 16: 5-HT$_{2A}$R signaling at E10.5-E11.5 does not mediate Isl1/2+ cell number. **(A)** The Number of visceral motor neurons (Isl1/1+) are quantified in control (cyan) and M100907 (magenta) cultures for 6 pairs of E10.5 + 1DIV hindbrains. **(B)** The number of Isl1/2+ cells in M100907 cultures is on average 96% of the Isl1/2+ cell in paired control cultures. Average is shown by horizontal line.

Expression of 5-HT$_{2A}$ receptor in p3 progenitor and 5-HT+ populations

Now that the effects of 5-HT$_{2A}$R signaling on SA and 5-HT+ cells have been documented, the question remains as to which cell types express this receptor. While many 5-HT cells have already been born by the beginning state for the cultures, E10.5, the monoamine is not yet detectable via immunohistochemistry (Figure 17). The 5-HT$_{2A}$R protein is also not detectable. However, we are able to identify the p3 progenitor population with Nkx2.2 and Foxa2 labels at this stage.

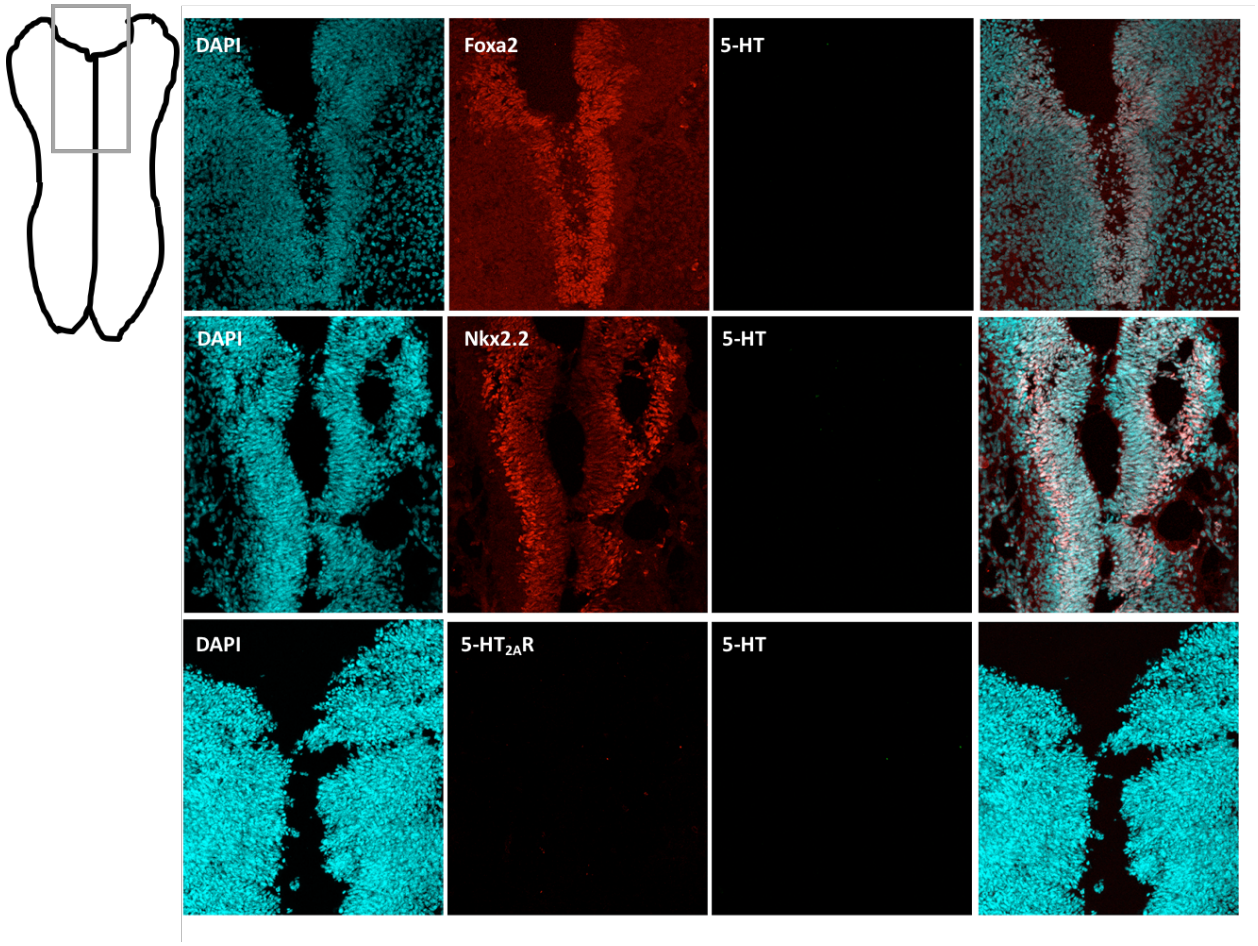

Figure 17: 5-HT monoamines and 5-HT$_{2A}$R protein are not detected at E10.5. This is the beginning state of the cultures. Neither 5-HT nor the 5-HT$_{2A}$ receptor are detected in the hindbrain. Region of focus within rostral hindbrain is depicted to the left. Each row displays a different 30 µm thick hindbrain section at 20x magnification. DAPI = nuclear marker; Nkx2.2 and Foxa2= progenitor markers.

By the end state of the cultures, E11.5, the 5-HT$_{2A}$R protein has a widespread distribution across the hindbrain, with robust signal around the midline and p3 domain (Figure 18). The developing 5-HT population is identifiable by 5-HT immunostain at this stage. SA is also occurring at this stage.

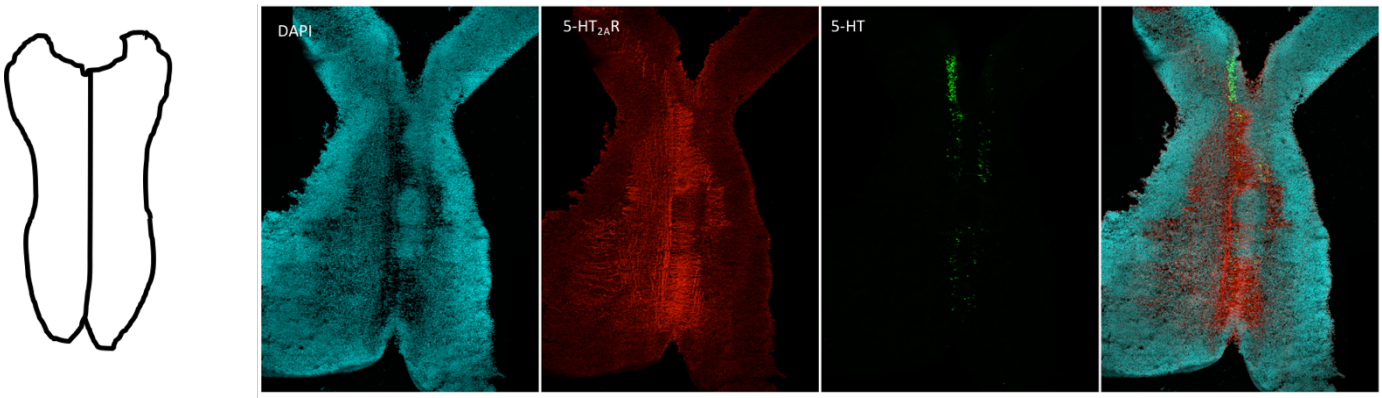

Fig 18: 5-HT and 5-HT$_{2A}$R are present in E11.5 hindbrains. This is the end state of the cultures, when waves of SA are also present. Both 5-HT and 5-HT$_{2A}$R signals are detected around the ventral midline. Image above features a 30 μm transverse cryosection through the hindbrain (hindbrain depicted by outline on the left) at 10x magnification.

Figure 19 shows serial sections of hindbrains stained for p3 progenitors and the 5-HT$_{2A}$ receptor at E11.5. Each antibody pictured in red was generated in mouse and could not be used within the

same hindbrain sections. We stained sequential slices in the hindbrain to show the p3 progenitors markers, 5-HT, and the 5-HT2A receptor protein all localize within the same general area.

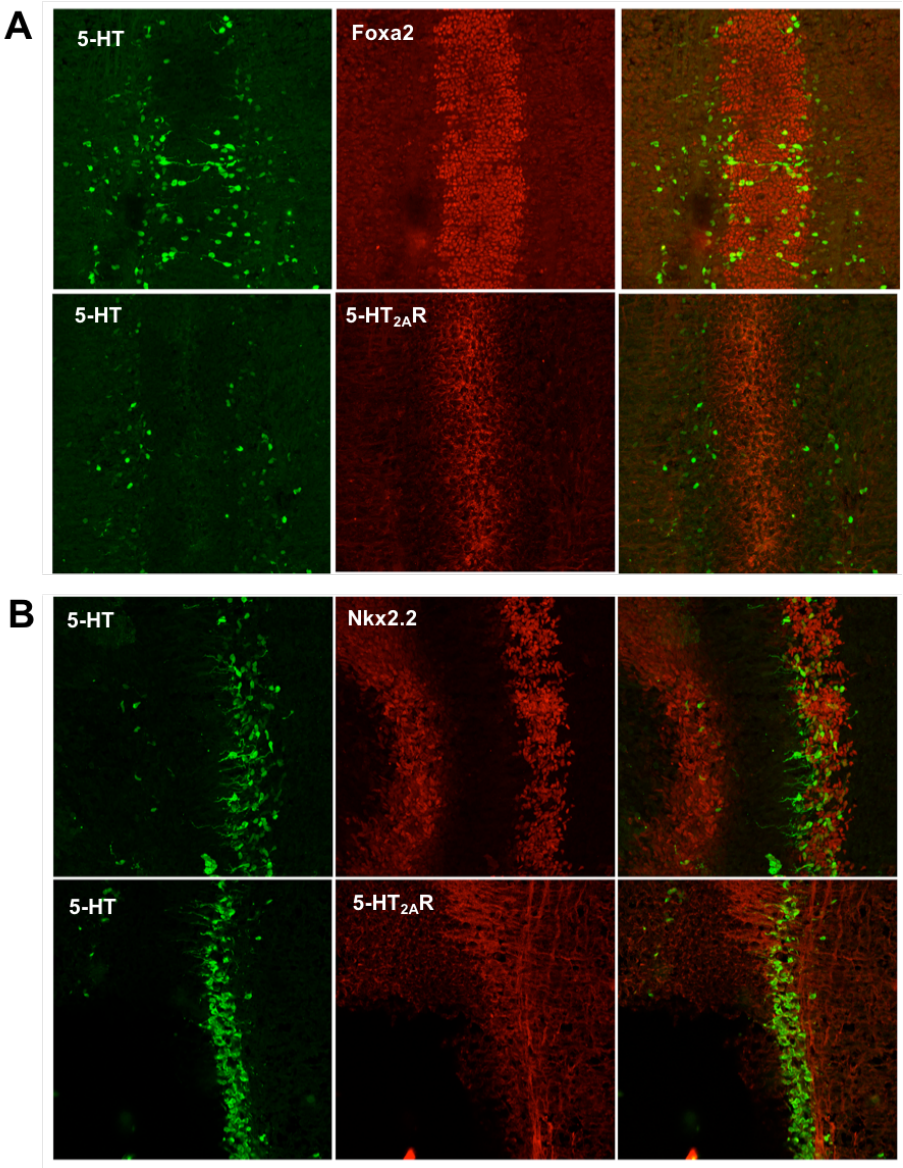

Figure 19: 5-HT$_{2A}$R is present in the p3 domain by the end of the culture period (E11.5). 5-HT and 5-HT$_{2A}$R signal is in same region as both p3 progenitor markers Foax2 **(A)** and Nkx2.2 **(B)**, as well as 5-HT. Each row displays a 30 µm section of the rostral hindbrain at 20x magnification.

The staining pattern of the 5-HT_{2A} receptor does not completely overlap with any other marker tested. Therefore, while immunostaining has been able to help verify the protein is present in the appropriate regions during the time of neurogenesis and SA, it has not helped to determine which specific cell types express the protein.

IV. Discussion and Future Directions

We hypothesized 5-HT released from developing raphe neurons promotes neural excitability in midline cells during circuit formation through activation of the 5-HT_2 family of receptors. Pharmacological data from this dissertation supports a central role of 5-HT_{2A} signaling in mediating spontaneous wave activity in the hindbrain (Figure 9). However, the onset of midline wave activity in the hindbrain (E11.5) is only 24 hours after differentiation begins for rostral 5-HT neurons. 5-HT axons have not yet reached their targets, meaning no mature 5-HT synapses have yet formed. For 5-HT to mediate spontaneous wave activity, 5-HT would have to be released from the newly born raphe cells. Deneris & Gaspar report that upon birth, 5-HT neurons immediately become polarized with growing axons that can release 5-HT from growth cones (2018). The genes necessary for presynaptic machinery and vesicular packaging of 5-HT are expressed in the hindbrain by E11.5 (Allen Brain Atlas). 5-HT is abundant throughout the neurons at this time, as is known through immunohistochemistry (Figure 4). Therefore, it is possible 5-HT is released by the developing neurons to mediate spontaneous activity through non-synaptic means.

There is evidence supporting non-synaptic release of 5-HT in the adult brain. Packaged vesicles of 5-HT are found in somas, axons and dendrites of presynaptic neurons without compatible postsynaptic receptors available (De-Miguel and Trueta 2005). 5-HT can also be detected through carbon fiber amperometry far from release sites when stimulating raphe neurons,

suggesting 5-HT molecules can diffuse to distant receptors (Bunin and Whiteman 1998). These reports support the idea that 5-HT could be released in the hindbrain extrasynaptically.

Acute 5-HT$_{2A}$ receptor blockade suppresses hindbrain spontaneous wave activity

This dissertation used more selective antagonists than previous publications to identify the specific receptor subtype involved in mediating SA. In acute Ca^{2+} imaging experiments, the antagonist specific to the 5-HT$_{2A}$ receptor, M100907, consistently stopped activity, and not antagonists to the 5-HT$_{2C}$. The 5-HT$_3$ receptor significantly decreased the frequency of SA but did not stop all events. The 5-HT$_{2A}$ receptor is an excitatory GPCR that has been shown to have a depolarizing effect on neuronal membrane potential.

Interestingly, while in acute experiments 5-HT$_{2A}$ receptor antagonists arrested all SA, M100907 did not do so in culture experiments. The Ca^{2+} imaging experiments were conducted using normal ACSF, providing opportunity for the drug to wash off. Under these conditions, the M100907 cultures exhibited SA frequencies similar to culture controls. This effect may be similar to the acute experiments in that the drug effects also wash off when normal ASCF is applied. While these M100907 cultures have a reduced number of 5-HT cells, 50% of the rostral 5-HT population remains intact, which must provide enough 5-HT for SA to continue in the absence of the antagonist.

Chronic 5-HT$_{2A}$ receptor blockade reduces serotonin cell number

We established a novel culture paradigm to test the hypothesis that prolonged exposure to 5-HT$_{2A}$ antagonists altered the morphology of developing hindbrain neurons. At the onset of cultures, hindbrains have no SA and no 5-HT+ neurons. After 24 hours, cultured hindbrains experienced the same patterns of midline SA as acute brains, at a slightly slower frequency (Figure 11). The cultured hindbrains also developed 5-HT+ neurons (Figure 12). The 5-HT rostral

population of neurons exhibited a 37.4% reduction in cell numbers in response to long-term exposure to the 5-HT_{2A} receptor antagonist M100907. This reduction only occurred during the window of 5-HT rostral neurogenesis for r2-3, and not in cultures one day older. The reduction also appears specific to the 5-HT+ population, as no reduction is observed in the visceral motor neurons born at similar times by the same progenitors. No reductions were found when SA was blocked independently of 5-HT_{2A} signaling with Mibefradil. These data support a novel role of 5-HT_{2A} signaling in mediating 5-HT+ cell number. However, the mechanism of regulation is unknown. 5-HT has been shown to regulate many developmental processes *in vitro*, including cell differentiation and death.

There are 3 possible stages of 5-HT development affected by the loss of 5-HT_{2A} signaling: specification, differentiation and death. Identifying the cell type expressing the receptor would help determine the developmental stage involved. To affect the progeny created by p3 progenitors, 5-HT_{2A} signaling would act through p3 progenitors that produce 5-HT_{2A} receptor mRNA. The existing 5-HT+ cells in r1 that are releasing 5-HT by E10.5 would have to be regulating progenitors in neighboring rhombomeres during the next wave of neurogenesis from E10.5-11.5. A "stop" signal must also exist to prevent 5-HT from stimulating endless production of 5-HT neurons. ISH for early serotonergic markers, like Pet1 and Lmx1b (Figure 6), in each culture condition would help determine if less 5-HT precursors are specified in response to M100907, as no reliable commercially available antibodies exist for these early markers.

In the second scenario, 5-HT precursor differentiation is stalled prior to 5-HT production, leaving precursor cells undetected by 5-HT immunostaining. Incomplete differentiation in response to altered 5-HT_{2A} signaling would require the precursors to express the receptor mRNA. To affect differentiation, r1 raphe neurons that release 5-HT would influence the maturation of

r2-3 raphe neurons. This scenario suggests the existence of two distinct subpopulations of rostral 5-HT+ neurons.

The last option is that the lack of 5-HT_{2A} signaling induces cell death, as an increase in dying cells could result in the observed cell reduction. Immunostaining for activated caspase 3 (AC3)+ cells that co-express 5-HT would help determine if more 5-HT+ cells are dying in the drug-treated cultures. The data in this dissertation have not ruled out cell death as a possible mechanism for the 5-HT cell reduction.

A big step in determining the mechanism for the 5-HT+ cell reduction is to identify the cells expressing the 5-HT_{2A} receptor that are targeted by M100907. 5-HT receptor antibodies are notoriously nonspecific (Weber & Andrade, 2010). However, Allen brain atlas ISH shows mRNA is present in the hindbrain by E11.5. This, paired with the pharmacology data showing a 5-HT_{2A} receptor effect, supports the notion that functional protein is present. The cell type expressing the 5-HT_{2A} receptor could be identified through fluorescent ISH (FISH). ISH for the 5-HT_{2A}R mRNA could be overlapped with staining from reliable antibodies for progenitor markers and 5-HT. This would provide more conclusive evidence as to which population is targeted by 5-HT_{2A}R antagonists.

This dissertation highlights two important roles for 5-HT_{2A}R signaling in hindbrain development. One is in generating waves of SA in the hindbrain, as all spontaneous waves stop during acute application of 5-HT_{2A}R-specific antagonists. Additionally, we provide evidence for a novel application of 5-HT as a morphogen in neural development. Chronic blockade of 5-HT_{2A}R reduces the number of serotonin cells in the hindbrain.

References

Alonso, A., Merchan, P., Sandoval, J., Sanchez-Arrones, L., Garcia-Cazorla, A., Artuch, R., Ferran, J., Martinez-de-la-Torre, M., Puelles, L. (2013). Development of the serotonergic cells in murine raphe nuclei and their relations with rhombomeric domains. *Brain Struct Funct*, *218*, 1229–1277.

Alves, S. E., Hoskin, E., Lee, S. J., Brake, W. G., Ferguson, D., Luine, V., … McEwen, B. S. (2002). Serotonin mediates CA1 spine density but is not crucial for ovarian steroid regulation of synaptic plasticity in the adult rat dorsal hippocampus. *Synapse*, *45*(2), 143–151.

Barr, A. M., Lehmann-Masten, V., Paulus, M., Gainetdinov, R. R., Caron, M. G., & Geyer, M. A. (2004). The Selective Serotonin-2A Receptor Antagonist M100907 Reverses Behavioral Deficits in Dopamine Transporter Knockout Mice. *Neuropsychopharmacology*, *29*(2), 221–228.

Blankenship, A. G., & Feller, M. B. (2009). Mechanisms underlying spontaneous patterned activity in developing neural circuits. *Nature Reviews Neuroscience*, *11*(1), 18–29.

Bonilla, S., Hall, A. C., Pinto, L., Attardo, A., Götz, M., Huttner, W. B., & Arenas, E. (2008). Identification of midbrain floor plate radial glia-like cells as dopaminergic progenitors. *Glia*, *56*(8), 809–820.

Bonnin, Goeden, Chen, Wilson, King, Shih, … Levitt. (2011). A transient placental source of serotonin for the fetal forebrain. *Nature*, *472*(7343), 347–350.

Bonnin, & Levitt. (2011). Fetal, maternal, and placental sources of serotonin and new implications for developmental programming of the brain. *Neuroscience*. *197*, 1-7.

Bortone, D., & Polleux, F. (2009). KCC2 Expression Promotes the Termination of Cortical Interneuron Migration in a Voltage-Sensitive Calcium-Dependent Manner. *Neuron*. *62*, 53-

71.

Bosma, M. M. (2010). Timing and mechanism of a window of spontaneous activity in embryonic mouse hindbrain development. *Annals of the New York Academy of Sciences*, *1198*(1), 182–191.

Bou-Flores, C., Lajard, A. M., Monteau, R., De Maeyer, E., Seif, I., Lanoir, J., … Mori, N. (2000). Abnormal Phrenic Motoneuron Activity and Morphology in Neonatal Monoamine Oxidase A-Deficient Transgenic Mice: Possible Role of a Serotonin Excess. *The Journal of Neuroscience*, *20*(12), 4646–4656.

Briscoe, J., Sussel, L., Serup, P., Hartigan-O'Connor, D., Jessell, T. M., Rubenstein, J. L. R., & Ericson, J. (1999). Homeobox gene Nkx2.2 and specification of neuronal identity by graded Sonic hedgehog signalling. *Nature*, *398*(6728), 622–627.

Canli, T., & Lesch, K. P. (2007). Long story short: The serotonin transporter in emotion regulation and social cognition. *Nature Neuroscience*, *10*(9), 1103–1109.

Cases, O., Lebrand, C., Giros, B., Vitalis, T., De Maeyer, E., Caron, M. G., … Seif, I. (1998). Plasma membrane transporters of serotonin, dopamine, and norepinephrine mediate serotonin accumulation in atypical locations in the developing brain of monoamine oxidase A knock-outs. *J Neurosci*, *18*(17), 6914–6927.

Cases, O., Seif, I., Grimsby, J., Gaspar, P., Chen, K., Pournin, S., … De Maeyer, E. (1995). Aggressive behavior and altered amounts of brain serotonin and norepinephrine in mice lacking MAOA. *Science*, *268*(5218), 1763–1766.

Cheng, L., Chen, C.-L., Luo, P., Tan, M., Qiu, M., Johnson, R., & Ma, Q. (2003). Lmx1b, Pet-1, and Nkx2.2 coordinately specify serotonergic neurotransmitter phenotype. *The Journal of Neuroscience : The Official Journal of the Society for Neuroscience*, *23*(31), 9961–7.

Daubert, E. A., & Condron, B. G. (2010). Serotonin: A regulator of neuronal morphology and circuitry. *Trends in Neurosciences*, *33*(9), 424–434.

De Lima, A. D., Gieseler, A., & Voigt, T. (2009). Relationship between GABAergic interneurons migration and early neocortical network activity. *Developmental Neurobiology*, *69*(2–3), 105–123.

Demarque, M., & Spitzer, N. C. (2010). Activity-dependent expression of Lmx1b regulates specification of serotonergic neurons modulating swimming behavior. *Neuron*. *67*, 321-334.

Deneris, & Gaspar. (2018). Serotonin neuron development: shaping molecular and structural identities. *Wiley Interdisciplinary Reviews: Developmental Biology*, *7*(1), 11–16.

Deneris, & Wyler. (2012). Serotonergic transcriptional networks and potential importance to mental health. *Nature Neuroscience*. *15*(4), 519-527.

Donahue, T. J., Hillhouse, T. M., Webster, K. A., Young, R., Oliveira, E. O. De, & Porter, J. H. (2017). Discriminative stimulus properties of the atypical antipsychotic amisulpride : comparison to its isomers and to other benzamide derivatives , antipsychotic , antidepressant , and antianxiety drugs in C57BL / 6 mice mice. *Psychopharmacology*, *234*, 3507–3520.

Easton, C. R., Dickey, C. W., Moen, S. P., Neuzil, K. E., Barger, Z., Anderson, T. M., … Hevner, R. F. (2015). Distinct Calcium Signals in Developing Cortical Interneurons Persist Despite Disorganization of Cortex by Tbr1 KO, *76*(7), 705–720.

Easton, C. R., Weir, K., Scott, A., Moen, S. P., Barger, Z., Folch, A., … Moody, W. J. (2014). Genetic Elimination of GABAergic Neurotransmission Reveals Two Distinct Pacemakers for Spontaneous Waves of Activity in the Developing Mouse Cortex. *Journal of Neuroscience*, *34*(11), 3854–3863.

Ever, L., & Gaiano, N. (2005). Radial “glial” progenitors: Neurogenesis and signaling. *Current*

Opinion in Neurobiology, *15*(1), 29–33.

Fiorica-Howells, E., Hen, R., Gingrich, J., Li, Z., & Gershon, M. D. (2002). 5-HT $_{2A}$ receptors: location and functional analysis in intestines of wild-type and 5-HT $_{2A}$ knockout mice. *American Journal of Physiology - Gastrointestinal and Liver Physiology*, *282*(5), G877–G893.

González-Maeso, J., Weisstaub, N. V., Zhou, M., Chan, P., Ivic, L., Ang, R., … Gingrich, J. A. (2007). Hallucinogens Recruit Specific Cortical 5-HT2AReceptor-Mediated Signaling Pathways to Affect Behavior. *Neuron*, *53*(3), 439–452.

Graham, A., Butts, T., Lumsden, A., & Kiecker, C. (2014). What can vertebrates tell us about segmentation? *EvoDevo*, *5*(1), 1–8.

Guiard, B. P., & Di Giovanni, G. (2015). Central serotonin-2A (5-HT2A) receptor dysfunction in depression and epilepsy: The missing link? *Frontiers in Pharmacology*, *6*(3), 1–17.

Gust, J., Wright, J. J., Pratt, E. B., & Bosma, M. M. (2003). Development of synchronized activity of cranial motor neurons in the segmented embryonic mouse hindbrain. *The Journal of Physiology*, *550*(Pt 1), 123–133.

Hansson, S. R., Mezey, E., & Hoffman, B. J. (1998). Serotonin transporter messenger RNA in the developing rat brain: early expression in serotonergic neurons and transient expression in non-serotonergic neurons. *Neuroscience*, *83*(4), 1185–1201.

Haugas, M., Tikker, L., Achim, K., Salminen, M., & Partanen, J. (2016). Gata2 and Gata3 regulate the differentiation of serotonergic and glutamatergic neuron subtypes of the dorsal raphe. *Development*, *143*(23), 4495–4508.

Hendricks, T., Francis, N., Fyodorov, D., & Deneris, E. S. (1999). The ETS domain factor Pet-1 is an early and precise marker of central serotonin neurons and interacts with a conserved

element in serotonergic genes. *The Journal of Neuroscience : The Official Journal of the Society for Neuroscience*, *19*(23), 10348–10356.

Hendricks, T. J., Fyodorov, D. V., Wegman, L. J., Lelutiu, N. B., Pehek, E. A., Yamamoto, B., … Deneris, E. S. (2003). Pet-1 ETS gene plays a critical role in 5-HT neuron development and is required for normal anxiety-like and aggressive behavior. *Neuron*, *37*(2), 233–247.

Hunt, Gust, McCabe, & Bosma. (2006). Primary role of the serotonergic midline system in synchronized spontaneous activity during development of the embryonic mouse hindbrain. *Journal of Neurobiology*, *66*(11), 1239–1252.

Hunt, Mccabe, & Bosma. (2005). Midline serotonergic neurones contribute to widespread synchronized activity in embryonic mouse hindbrain. *J Physiol*, *5663*, 807–819.

Hunt, McCabe, & Bosma. (2005). Midline serotonergic neurones contribute to widespread synchronized activity in embryonic mouse hindbrain. *The Journal of Physiology*, *566*(Pt 3), 807–819.

Jacob, J., Ferri, A. L., Milton, C., Prin, F., Pla, P., Lin, W., … Briscoe, J. (2007). Transcriptional repression coordinates the temporal switch from motor to serotonergic neurogenesis. *Nature Neuroscience*, *10*(11), 1433–1439.

Jessell, T. M. (2000). Neuronal specification in the spinal cord: Inductive signals and transcriptional codes. *Nature Reviews Genetics*, *1*(1), 20–29.

Kasper, J., Booth, R., & Peris, J. (2015). Serotonin-2C Receptor Agonists Decrease Potassium-Stimulated GABA Release In the Nucleus Accumbens. *Synapse*, *69*(2), 78–85.

Kastanenka, K. V, & Landmesser, L. T. (2013). Optogenetic-mediated increases in in vivo spontaneous activity disrupt pool-specific but not dorsal-ventral motoneuron pathfinding. *Proceedings of the National Academy of Sciences of the United States of America*, *110*(43),

17528–17533.

Kehne, J., Baron, B., Carr, A., Chaney, F., Elands, J., Johnson, M., … Widmaier, C. (1996). Preclinical Characterization of the Potential of the Putative Atypical Antipsychotic MDL 100907 with a Favorable CNS Safety Profile. *The Journal of Pharmacology and Experimental Therapeutics*, *277*, 968–981.

Kingsbury, B. F. (1920). The Developmental Origin of the Notochord. *Science*, *51*(1312), 190 - 193.

Kiyasova, V., Fernandez, S. P., Laine, J., Stankovski, L., Muzerelle, A., Doly, S., & Gaspar, P. (2011). A Genetically Defined Morphologically and Functionally Unique Subset of 5-HT Neurons in the Mouse Raphe Nuclei. *Journal of Neuroscience*, *31*(8), 2756–2768.

Kiyasova, V., & Gaspar, P. (2011). Development of raphe serotonin neurons from specification to guidance. *European Journal of Neuroscience*. *34*, 1553-1562.

Komuro, H., & Rakic, P. (1996). Intracellular Ca2+ Fluctuations Modulate the Rate of Neuronal Migration. *Neuron*, *17*(2), 275–285.

Lauder, J. M., Tamir, H., & Sadler, T. W. (1988). Serotonin and morphogenesis. *Development*, *102*, 709–720.

Lavdas, a a, Blue, M. E., Lincoln, J., & Parnavelas, J. G. (1997). Serotonin promotes the differentiation of glutamate neurons in organotypic slice cultures of the developing cerebral cortex. *The Journal of Neuroscience : The Official Journal of the Society for Neuroscience*, *17*(20), 7872–80.

Lebrand, C., Cases, O., Wehrlé, R., Blakely, R. D., Edwards, R. H., & Gaspar, P. (1998). Transient developmental expression of monoamine transporters in the rodent forebrain. *Journal of Comparative Neurology*, *401*(4), 506–524.

Lesch, K. P., & Waider, J. (2012). Serotonin in the Modulation of Neural Plasticity and Networks: Implications for Neurodevelopmental Disorders. *Neuron*. 76(175-191).

Lieske, V., Bennett-Clarke, C. A., & Rhoades, R. W. (1999). Effects of serotonin on neurite outgrowth from thalamic neurons in vitro. *Neuroscience*, *90*(3), 967–974.

Lischalk, J. W., Easton, C. R., & Moody, W. J. (2009). Bilaterally propagating waves of spontaneous activity arising from discrete pacemakers in the neonatal mouse cerebral cortex. *Developmental Neurobiology*, *69*(7), 407–414.

Liu, J., & Lauder, J. M. (1991). Serotonin and nialamide differentially regulate survival and growth of cultured serotoni and catecholamine neurons. *Developmental Brain Research*, *60*, 59–67.

Lobo. (2008). Birth Defects: Prevention and Treatment. Retrieved from https://www.nature.com/scitable/topicpage/birth-defects-prevention-and-treatment-859

McCabe, A. K., Easton, C. R., Lischalk, J. W., & Moody, W. J. (2007). Roles of glutamate and GABA receptors in setting the developmental timing of spontaneous synchronized activity in the developing mouse cortex. *Developmental Neurobiology*, *67*(12), 1574–1588.

Meister, M., Wong, R. O., Baylor, D. A., & Shatz, C. J. (1991). Synchronous bursts of action potentials in ganglion cells of the developing mammalian retina. *Science*, *252*(5008), 939–43.

Moens, C. B., & Prince, V. E. (2002). Constructing the hindbrain: Insights from the zebrafish. *Developmental Dynamics*, *224*(1), 1–17.

Moiseiwitsch, J. R., & Lauder, J. M. (1995). Serotonin regulates mouse cranial neural crest migration. *Proceedings of the National Academy of Sciences of the United States of America*, *92*(16), 7182–7186.

Momose-Sato, Y., Nakamori, T., & Sato, K. (2012). Spontaneous depolarization wave in the

mouse embryo: Origin and large-scale propagation over the CNS identified with voltage-sensitive dye imaging. *European Journal of Neuroscience*, *35*(8), 1230–1241.

Moody, W. J., & Bosma, M. M. (2005). Ion channel development, spontaneous activity, and activity-dependent development in nerve and muscle cells. *Physiol Rev.*, *85*(0031–9333 (Print)), 883–941.

Moruzzi, A. M., Abedini, N. C., Hansen, M. A., Olson, J. E., & Bosma, M. M. (2009). Differential expression of membrane conductances underlies spontaneous event initiation by rostral midline neurons in the embryonic mouse hindbrain. *Journal of Physiology*, *587*(21), 5081–5093.

Muller, Anacker, Rogers, Goeden, Keller, Forsberg, … Veenstra-Vanderweele. (2017). Impact of Maternal Serotonin Transporter Genotype on Placental Serotonin, Fetal Forebrain Serotonin, and Neurodevelopment. *Neuropsychopharmacology*, *42*(2), 427–436.

Nicholls, J. G., Martin, A. R., Wallace, B. G., & Fuchs, P. A. (2001). *From Neuron to Brain: A Cellular and Molecular Approach to the Function of the Nervous System, Fourth Edition*.

Nolte, C., & Krumlauf, R. (2007). Expression of Hox genes in the nervous system of vertebrates. *HOX Gene Expression*. http://doi.org/10.1007/978-0-387-68990-6_2

Norrholm, S. D., & Ouimet, C. C. (2000). Chronic fluoxetine administration to juvenile rats prevents age-associated dendritic spine proliferation in hippocampus. *Brain Research*, *883*(2), 205–215.

Nouri, N., Patel, M. J., Joksimovic, M., Poulin, J. F., Anderegg, A., Taketo, M. M., … Awatramani, R. (2015). Excessive Wnt/beta-catenin signaling promotes midbrain floor plate neurogenesis, but results in vacillating dopamine progenitors. *Molecular and Cellular Neuroscience*, *68*, 131–142.

Numakawa, T., Suzuki, S., Kumamaru, E., Adachi, N., Richards, M., & Kunugi, H. (2010). BDNF function and intracellular signaling in neurons. *Histology and Histopathology*, *25*(2), 237–258.

Ono, Y., Nakatani, T., Sakamoto, Y., Mizuhara, E., Minaki, Y., Kumai, M., … Imai, T. (2007). Differences in neurogenic potential in floor plate cells along an anteroposterior location: midbrain dopaminergic neurons originate from mesencephalic floor plate cells. *Development*, *134*(17), 3213–3225.

Pattyn, A., Simplicio, N., van Doorninck, J. H., Goridis, C., Guillemot, F., & Brunet, J. F. (2004). Ascl1/Mash1 is required for the development of central serotonergic neurons. *Nat Neurosci*, *7*(6), 589–595.

Persico, A. M., Baldi, A., Dell'Acqua, M. L., Moessner, R., Murphy, D. L., Lesch, K. P., & Keller, F. (2003). Reduced programmed cell death in brains of serotonin transporter knockout mice. *NeuroReport*, *14*(3), 341–344.

Persico, A. M., Di Pino, G., & Levitt, P. (2006). Multiple receptors mediate the trophic effects of serotonin on ventroposterior thalamic neurons in vitro. *Brain Research*, *1095*(1), 17–25.

Philippidou, P., & Dasen, J. (2013). Hox Genes: Choreographers in Neural Development, Architects of Circuit Organization. *Neuron*, *80*(1), 247–253.

Ribes, V., & Briscoe, J. (2009). Establishing and interpreting graded Sonic Hedgehog signaling during vertebrate neural tube patterning: the role of negative feedback. *Cold Spring Harbor Perspectives in Biology*, *1*(2), 1–17.

Rios, M., Lambe, E., Liu, R., Teillon, S., Liu, J., Akbarian, S., … Aghajanian, G. (2006). Severe Deficits in 5-HT2A-Mediated Neurotransmission in BDNF Conditional Mutant Mice. *Journal of Neurobiology*, *66*(January), 408–420.

Sanes, D. H., Reh, T. A., & Harris, W. A. (2012). *Development of the Nervous System* (3rd Editio). Burlington: Elsevier Inc.

Shatz, C. J., & Stryker, M. P. (1988). Prenatal tetrodotoxin infusion blocks segregation of retinogeniculate afferents. *Science*, *242*(4875), 87–89.

Shen, K.-Z., Kozell, L. B., & Johnson, S. W. (2007). Multiple conductances are modulated by 5-HT receptor subtypes in rat subthalamic nucleus neurons. *Neuroscience*, *148*(4), 996–1003.

Shih, J. C., Ridd, M. J., Chen, K., Meehan, W. P., Kung, M. P., Seif, I., & De Maeyer, E. (1999). Ketanserin and tetrabenazine abolish aggression in mice lacking monoamine oxidase A. *Brain Research*, *835*(2), 104–112.

Smidt, M. P., & van Hooft, J. a. (2013). Subset specification of central serotonergic neurons. *Frontiers in Cellular Neuroscience*, *7*(200), 1-7.

Stankovski, L., Alvarez, C., Ouimet, T., Vitalis, T., El-Hachimi, K. H., Price, D., … Cases, O. (2007). Developmental Cell Death Is Enhanced in the Cerebral Cortex of Mice Lacking the Brain Vesicular Monoamine Transporter. *Journal of Neuroscience*, *27*(6), 1315–1324.

Sturgeon, K., Kaneko, T., Biemann, M., Gauthier, A., Chawengsaksophak, K., & Cordes, S. P. (2011). Cdx1 refines positional identity of the vertebrate hindbrain by directly repressing Mafb expression. *Development*, *138*(1), 65–74.

Upton, a L., Salichon, N., Lebrand, C., Ravary, a, Blakely, R., Seif, I., & Gaspar, P. (1999). Excess of serotonin (5-HT) alters the segregation of ispilateral and contralateral retinal projections in monoamine oxidase A knock-out mice: possible role of 5-HT uptake in retinal ganglion cells during development. *The Journal of Neuroscience : The Official Journal of the Society for Neuroscience*, *19*(16), 7007–7024.

Vaidya, V. a, Marek, G. J., Aghajanian, G. K., & Duman, R. S. (1997). 5-HT2A receptor-mediated

regulation of brain-derived neurotrophic factor mRNA in the hippocampus and the neocortex. *The Journal of Neuroscience*, *17*(8), 2785–2795.

Vitalis, T., Cases, O., Gillies, K., Hanoun, N., Hamon, M., Seif, I., … Price, D. J. (2002). Interactions between TrkB Signaling and Serotonin Excess in the Developing Murine Somatosensory Cortex: A Role in Tangential and Radial Organization of Thalamocortical Axons. *The Journal of Neuroscience*, *22*(12), 4987 -5000.

Vitalis, T., & Parnavelas, J. G. (2003). The role of serotonin in early cortical development. *Developmental Neuroscience*. *25*, 245-156.

Ward, R., Pediani, J., Godin, A., & Milligan, G. (2015). Regulation of Oligomeric Organization of the Serotonin 5-Hydroxytryptamine 2C (5-HT 2C) Receptor Observed by Spatial Intensity Distribution Analysis *. *The Journal of Biological Chemistry*, *290*(20), 12844–12857.

Watari, H., Tose, A. J., & Bosma, M. M. (2013). Hyperpolarization of resting membrane potential causes retraction of spontaneous $Ca(i)^{2+}$ transients during mouse embryonic circuit development. *The Journal of Physiology*, *591*(Pt 4), 973–83.

Weisstaub, N. V. (2006). Cortical 5-HT2A Receptor Signaling Modulates Anxiety-Like Behaviors in Mice. *Science*, *313*(5786), 536–540.

Wirth, A., Holst, K., & Ponimaskin, E. (2016). How serotonin receptors regulate morphogenic signalling in neurons. *Progress in Neurobiology*.

Yang, J.-W., Hanganu-Opatz, I. L., Sun, J.-J., & Luhmann, H. J. (2009). Three Patterns of Oscillatory Activity Differentially Synchronize Developing Neocortical Networks In Vivo. *Journal of Neuroscience*, *29*(28), 9011–9025.

Ybot-Gonzalez, P., Gaston-Massuet, C., Girdler, G., Klingensmith, J., Arkell, R., Greene, N. D. E., & Copp, A. J. (2007). Neural plate morphogenesis during mouse neurulation is regulated

by antagonism of Bmp signalling. *Development*, *134*(17), 3203–3211.

Zhao, Z.-Q., Scott, M., Chiechio, S., Wang, J.-S., Renner, K. J., Gereau, R. W., … Chen, Z.-F. (2006). Lmx1b Is Required for Maintenance of Central Serotonergic Neurons and Mice Lacking Central Serotonergic System Exhibit Normal Locomotor Activity. *Journal of Neuroscience*, *26*(49), 12781–12788.

Table 1. Antibodies used in IHC.

Antibody against	**Species**	**Concentration**	**Vendor**
5-HT	mouse	1:1000	unknown
5-HT	rabbit	1:300	unknown
5-HT_{2A}R	mouse	1:250	BD Pharmingen
5-HT_{2C}R	mouse	1:250	BD Pharmingen
Nkx2.2	mouse	1:250	DSHB
Foxa2	mouse	1:250	DSHB
Isl1/2	mouse	1:50	DSHB